Acuren Group Inc.
12271 Horseshoe Way
Richmond, BC, Canada V7A 4V4
www.acuren.com

Phone: 604.275.3800
Fax: 604.274.7235

A Higher Level of Reliability

EXAMINATION OF FAILED COMPONENTS OF A CONSTRUCTION HOIST

Prepared for:

TALL CRANE EQUIPMENT LTD.
22652 FRASER HWY
LANGLEY TWP, BC V2Z 2T8

Copy to:
TECHNICAL SAFETY B.C.
600 - 2889 EAST 12TH AVENUE
VANCOUVER, BC
V5M 4T5

Attention: [redacted]

File Number: 60515067
Date: September 11, 2019

[redacted] P.Eng.
[redacted]@acuren.com
[redacted]

TABLE OF CONTENTS

LIST OF FIGURES

LIST OF TABLES

1.0 INTRODUCTION

A gear, a splined shaft and a gear rack section on a construction hoist all broke in service. Acuren was requested by Tall Crane Equipment Ltd. for assistance to determine the causes of these failures and for recommendations to inspect identical hoists to reduce the risk of similar failures.

The construction hoist consisted of three (3) identical drive gears (each has its own motor and reduction gear box) and a vertical gear rack. It was reported that:

1. The bottom gear of the original three gears suffered a broken tooth first.
2. A replacement gear was then installed on the bottom position, but the bottom gear shaft broke shortly after the gear replacement.
3. The gear rack was found broken during inspection of the broken shaft.

The service and maintenance history of the hoist was not provided for this examination.

The broken shaft, gear box, replacement gear, and the broken rack section (see **Figure 1**a) were submitted to Acuren for failure analysis. In addition, the three (3) original gears (top, middle and bottom, **Figure 1**b) were also submitted for examination.

The results of our analysis are as follows.

2.0 EXAMINATIONS

Figure 1 shows the hoist components as received. The broken shaft sections remained inside the gear box on the inboard side and the replacement gear on the outboard side. The rack section broke at one end. The bottom gear of the three (3) original gears suffered a broken tooth.

The name plate on the reduction gear box (see **Figure 2**) showed that it was made for construction hoists.

2.1 Broken Splined Shaft

2.1.1 Visual Examination

The bottom gear splined shaft broke between the gear box and the gear (see **Figure 3**). The outboard end of the shaft was intact (see **Figure 4**).

The broken shaft exhibited a star-shaped fracture (also see **Figure 3**). Detailed examination revealed coarse fatigue beach marks on the drive side of each spline (see **Figure 5**). These features are characteristics of a torsional fatigue failure of a splined shaft.

The fracture exhibited a fairly new appearance (see **Figure 3**a for clean fracture on the gear box side and **Figure 3**b for recently formed rust on the gear side). The light rust on the gear side fracture was readily removable by inhibited acid cleaning (see **Figure 6**). These fracture features indicated that the fatigue cracking on the splined shaft was fairly recent, perhaps within a couple of months.

The splined shaft section inside the gear was slightly rusted (see **Figure 7**a). The light rust was readily removable by inhibited acid cleaning (see **Figure 7**b). It is worthwhile noting that the splines exhibited a rough machining surface finish, particularly at the spline roots/fillets. The rough surface finish at the fatigue critical spline roots/fillets would have substantially reduced the fatigue resistance of the shaft.

2.1.2 Chemical Analysis of Shaft Steel

The steel of the shaft was subjected to a spark emission spectrometer chemical analysis. The results, together with the chemical composition specifications of Chinese GB/T 3077 Grades 40Cr and 45Cr, are listed in Table 1.

The shaft steel met the chemical specifications of both Grades 40Cr and Grade 45Cr steels. The shaft was most likely made from a GB/T 3077 Grade 40Cr chromium low alloy steel, because Grade 40Cr is more common than Grade 45Cr in China for shaft applications. The use of a medium carbon low alloy steel is deemed appropriate for the given application.

TABLE 1: CHEMICAL COMPOSITION OF SHAFT AND RELEVANT SPECIFICATIONS (WT%)

Element	Shaft	GB/T 3077 Gr. 40Cr	GB/T 3077 Gr. 45Cr
Carbon (C)	0.44	0.37 – 0.44	0.42 – 0.49
Silicon (Si)	0.26	0.17 – 0.37	0.17 – 0.37
Manganese (Mn)	0.60	0.50 – 0.80	0.50 – 0.80
Phosphorus (P)	0.018	0.035 max.	0.035 max.
Sulphur (S)	0.017	0.035 max.	0.035 max.
Chromium (Cr)	0.91	0.80 – 1.10	0.80 – 1.10
Nickel (Ni)	0.01	Not specified	Not specified
Molybdenum (Mo)	0.001	Not specified	Not specified
Aluminium (Al)	0.004	Not specified	Not specified
Copper (Cu)	0.006	Not specified	Not specified
Iron (Fe)	Balance	Balance	Balance

2.1.3 Metallographic Examination and Hardness Testing

A transverse cross-sectional metallographic specimen was prepared from the intact outboard end of the broken shaft for examination of its microstructure and testing of its hardness.

The shaft was found to be through-hardened (see **Figure 8**) with a quenched and tempered martensitic microstructure (see **Figure 9**).

Vickers microhardness tests performed on the metallographic specimen resulted in an average of 270 HV 500g, which is equivalent to 26 HRC. This hardness is considered to be in the range for a quenched and tempered Grade 40Cr steel for shaft applications. However, the manufacturer's specification needs to reviewed for the strength adequacy of the shaft.

2.2 Examination of Broken Rack

2.2.1 Visual Examination

The rack section was measured 1.5 meters long and it had one bolt hole on each end (see **Figure 10**). The rack on the hoist would have been made up of several such rack sections that were bolted on a rack frame.

The rack section broke through a bolt hole, as shown in **Figure 11**. Judging by the preferential wear on the driving side of the rack teeth (facing up or hoisting direction), the failure occurred at the lower bolt hole of this particular rack section.

The fracture had been severely damaged by rubbing between the mating fractures after the failure and the damaged fracture was covered with light rust (see **Figure 12**a). The rack had broken for some time before it was taken out from service. Despite damage, the fracture exhibited a clear brittle fracture pattern on a macro-scale which pointed back to origins along the root of the tooth (see **Figure 12**b).

The rack teeth away from the fractured location exhibited moderate material flow on the drive flanks and minor plastic flow on the non-drive flanks (see **Figure 13**a). A few teeth around the fracture sustained severe material flow on both the drive and non-drive flanks (see **Figure 13**b). The plastic flow on the drive flanks of the rack teeth was caused by loading from the gears that exceeded the yield strength of the rack steel. The severe plastic flow on both the drive and non-drive flanks of the teeth close to the rack fracture most likely occurred after the rack failure when the engagement with the gears was out-of-pitch.

The rack piece that broke away did not exhibit any evidence to suggest that the failure was caused by an impact from a construction object or tooling damage as shown in **Figure 14**.

2.2.2 Fractographic Examination

The cleaned fracture of the rack was examined using a scanning electron microscope (SEM).

The fracture was substantially damaged by rubbing against its mating fracture after the failure (see **Figure 15**). However, a few microscopic intact areas at the fracture origins were found to exhibit a clear transgranular brittle cleavage fracture pattern (see **Figure 16**). Such a fractographic pattern indicated that the fracture was caused by an impact on the rack tooth.

2.2.3 Non-destructive Testing

The entire rack section was inspected using a magnetic particle non-destructive inspection method (MPI) for cracks. This revealed linear indications along the roots of two teeth immediately adjacent to the fracture (see **Figure 17**). The nature of these indications was later examined metallographically.

No crack indications were observed on other teeth of the rack section.

2.2.4 Chemical Analysis of Rack Steel

The steel of the rack was subjected to a spark emission spectrometer chemical analysis. The results, together with the chemical composition specifications of Chinese GB/T 699 Grade 60 carbon steel and AISI Grade 1060, are listed in Table 2.

The rack steel met the chemical specification of Chinese GB/T 699 Grade 60 carbon steel, which is equivalent to AISI Grade 1060.

TABLE 2: CHEMICAL COMPOSITION OF RACK AND RELEVANT SPECIFICATIONS (WT%)

Element	Rack	GB/T 699 Gr. 60	AISI 1060
Carbon (C)	0.61	0.57 – 0.65	0.55 – 0.65
Silicon (Si)	0.37	0.17 – 0.37	Not specified
Manganese (Mn)	0.72	0.50 – 0.80	0.60 – 0.90
Phosphorus (P)	0.017	0.035 max.	0.040 max.
Sulphur (S)	0.023	0.035 max.	0.050 max.
Chromium (Cr)	0.09	0.25 max.	Not specified
Nickel (Ni)	0.07	0.30 max.	Not specified
Molybdenum (Mo)	0.005	Not specified	Not specified
Aluminium (Al)	0.005	Not specified	Not specified
Copper (Cu)	0.10	0.25 max.	Not specified
Iron (Fe)	Balance	Balance	Balance

2.2.5 Metallographic Examination and Hardness Testing

A metallographic specimen was prepared from the rack across the fracture through an origin, as previously shown in **Figure 12**, to examine the microstructure of the rack and the profile of the cracks at the neighbouring teeth.

Metallographic examination revealed that the rack exhibited a uniform microstructure throughout its teeth and body (see **Figure 18**). The microstructure of the rack consisted of a mixture of coarse-grained pearlite colonies and grain boundary ferrite (see **Figure 19**). These metallographic features indicated that the rack was machined out of a hot-rolled bar stock of GB/T 699 Grade 60 carbon steel.

The fracture was transgranular through the coarse grains with a zigzag path (see **Figure 20**). A large tooth crack also exhibited a similar profile (see

Figure 21). Given the brittle cleavage fracture pattern observed on the fracture, the large tooth root crack was also a brittle fracture by impact loads. The brittle cracking might have been generated by multiple impact loads, and the cracking advanced and then arrested during each impact event.

The hardness of the rack was tested to be 99 HRB, which is below 20 HRC. This low hardness was normal for a hot-rolled, coarse-grained GB/T 699 Grade 60 carbon steel.

The steel would be expected to have low fracture toughness and wear resistance. However, the choice of material might be reasonable for the given application, considering each individual tooth on the rack is subjected to less frequent loading than the gears. Nonetheless, the manufacturer's specification needs to reviewed for the material adequacy of the rack.

2.3 Examination of Gears

2.3.1 Visual Examination

The three (3) original gears are shown in **Figure 22** as received. The bottom gear suffered one broken tooth and the other two (2) gears were intact.

Other than the broken tooth on the bottom gear, these gears exhibited a similar wear pattern as shown in **Figure 23**. The teeth on all three gears showed engagement marks of 38 mm wide over the 48 mm tooth width starting from the inboard edge. The 48 mm wide gears would have been aligned with the 38 mm wide rack on the inboard edge. **Figure 24** illustrates the mismatching outboard side of the gear-rack engagement.

The gears all exhibited more severe wear and material flow on the drive side and minor wear on the non-drive side.

The replacement gear also exhibited a similar engagement pattern (see **Figure 25**). It exhibited a reasonable amount of grease on it, which indicates that it was lubricated.

All of the gears exhibited an involute tooth profile. Different from the original gears, the replacement gear exhibited a much smaller end round (see **Figure 26**). This indicated that the original gears and replacement gears were of different batches.

All of the gears exhibited a rough machining surface finish, particularly on the root land and fillet, which would be expected to adversely affect the fatigue resistance of the gears.

2.3.2 Magnetic Particle Inspection

All of the gears were subjected to magnetic particle inspection (MPI) for cracks along the tooth roots. They were all found to have linear indications along the tooth roots (see **Figure 27**).

2.3.3 Fractographic Examination of Broken Gear

The fracture of the broken tooth was along the tooth fillet (see **Figure 28**). The fracture was generally flat without apparent plastic deformation. It exhibited ratcheted marks along the edges on both the drive and non-drive sides of the tooth. These features are consistent with a reverse bending fatigue fracture that originated from multiple origins on both sides of the tooth.

The neighbouring tooth exhibited multiple cracks on the tooth fillet surface along the coarse machining lines (see **Figure 29**). The ratcheted pattern on the fracture of the broken tooth would have resulted from coalescence of multiple cracks similar to the secondary cracks on the neighbouring tooth.

The fracture on the drive side was severely damaged by rubbing against the opposing fracture surface (see **Figure 30**a). A small undamaged area along the edge of the fracture was found to have been severely corroded (see **Figure 30**b). The fracture on the non-drive side also exhibited similar mechanical and corrosion damage, except for less extent of corrosion (see **Figure 31**). The extent of corrosion on the gear fracture indicated that the cracking had occurred long ago.

No fractographic features could be identified for determination of the fracture mode on a microscopic scale.

Figure 32 shows SEM images of fillet cracks on the rough machined surface.

2.3.4 Chemical Analysis of Replacement Gear Steel

The steel of the replacement gear was subjected to a spark emission spectrometer chemical analysis. The results, together with the chemical composition specifications of Chinese GB/T 3077 Grade 35CrMo low alloy steel and AISI Grade 4135, are listed in Table 3.

The gear steel met the chemical specifications of Chinese GB/T 3077 Grade 35CrMo Cr-Mo low alloy steel, which is equivalent to AISI Grade 4135.

Low alloy steel and medium-carbon steels are typical choices for induction hardened gears. The use of a 0.35% carbon low alloy steel for an induction hardened hoist gears (see in metallographic examination) is considered low.

TABLE 3: CHEMICAL COMPOSITION OF REPLACEMENT GEAR AND RELEVANT SPECIFICATIONS (WT%)

Element	Gear	GB/T 3077 Gr. 35CrMo	AISI 4135
Carbon (C)	0.35	0.32 – 0.40	0.33 – 0.38
Silicon (Si)	0.24	0.17 – 0.37	0.15 – 0.30
Manganese (Mn)	0.52	0.40 – 0.70	0.70 – 0.90
Phosphorus (P)	0.020	0.035 max.	0.035 max.
Sulphur (S)	0.013	0.035 max.	0.040 max.
Chromium (Cr)	0.93	0.80 – 1.10	0.80 - 1.10
Nickel (Ni)	0.01	0.30 max.	Not specified
Molybdenum (Mo)	0.20	0.15 – 0.25	0.15 – 0.25
Aluminium (Al)	0.016	Not specified	Not specified
Copper (Cu)	0.02	0.25 max.	Not specified
Iron (Fe)	Balance	Balance	Balance

2.3.5 Metallographic Examination and Hardness Testing of Broken Gear

A metallographic specimen was prepared across the fracture of the broken tooth as well as two neighbouring teeth to examine the microstructure of the gear and the profile of the secondary cracks. Vickers microhardness testing was also performed on the gear. The following observations were made through these examination and testing.

1. The gear exhibited a flank-and-tooth-hardening pattern with the transition zone located at the fatigue critical tooth fillet areas (see **Figure 33**).

2. The gear body exhibited a quenched and tempered microstructure (a mixture of tempered martensite and bainite) with a relatively coarse grain size (see **Figure 34**). It appeared that the gear was machined out of a heat treated bar stock.

3. The tooth exhibited a mixture of very fine-grained ferrite and tempered martensite microstructure (see **Figure 35**). This indicated that the gear teeth were hardened by an induction hardening method, and that the heating failed to reach the single austenite phase temperature zone. This indicated that the induction tooth-hardening was performed with wrong process parameters.

4. The hardness of the gear tooth varied from 345 to 500 HV 500g, which is equivalent to 35 to 49 HRC (also see **Figure 33**).

5. The gear body has a hardness around 255 HV 500g or 23 HRC, which is considered low.

6. The lowest hardness was located at the transition zone at the fatigue critical tooth fillet area, being 190 to 220 HV 500g or below 20 HRC. This excessively low hardness would have significantly compromised the fatigue strength of the gear.

7. The cracks at the tooth fillet were found to be straight and transgranular at the tooth roots through the softest transition zone (see **Figure 33** and **Figure 36**). The profile of the cracks is consistent with fatigue cracks.

2.3.6 Metallographic Examination and Hardness Testing of Mid-Gear

A metallographic specimen was prepared from the original mid-gear across three (3) teeth.

Different from the broken gear, the mid-gear exhibited a uniform microstructure throughout the teeth and body (see **Figure 37**). This meant that the mid-gear was not induction tooth-hardened after machining.

The mid-gear exhibited a quenched and tempered microstructure including the tooth root areas (see **Figure 38**), with a consistent hardness of 350 HV 500g (equivalent to 36 HRC). The hardness on the flanks of the mid-gear is lower than the case-hardened zone of the broken gear, but is higher than the body of the broken gear. More importantly, the harness of the mid-gear at the tooth root is much harder than that of the broken gear.

The fillets of the gear teeth exhibited a rough machined surface profile resulting from aggressive machining (also see **Figure 38**).

2.3.7 Metallographic Examination and Hardness Testing of Replacement Gear

A metallographic specimen was prepared from the replacement gear across three (3) teeth. This revealed that the gear exhibited tooth-and-root hardening pattern (see **Figure 39**). The microstructure of the hardened zone, including the tooth root areas, consisted of a fine-grained tempered martensite microstructure (see **Figure 40**).

The hardness of the gear is 500 to 540 HV 500g (49 to 52 HRC) in the hardened zone (including the root area), and 220 to 240 HV 500g (20 HRC or below) in the transition zone 2 mm under the tooth root contour.

Despite hardening around the tooth roots, the replacement gear had developed multiple fatigue cracks just below the engaged flanks on both the drive and non-drive sides (also see **Figure 40**).

3.0 DISCUSSION

The results of this examination are summarized in Table 4. It is our opinion that:

1. The fatigue failure of the original bottom gear was caused by the use of a gear that is inadequate for the application.
2. The brittle failure of the rack section was caused by an impact load by the bottom gear after its tooth broke off.
3. The torsional fatigue cracking of the bottom gear shaft might have started fairly recently, after the original bottom gear suffered a broken tooth. The cracking continued after installation of the replacement gear, and the shaft ultimately broke a month later.

TABLE 4: SUMMARY OF FINDINGS

	Original gears			Replacement Gear	Shaft	Rack
	Bottom	Middle	Top			
Time in service	Unknown	Unknown	Unknown	Less than a month	Unknown	Unknown
Condition	Broken by fatigue racking at tooth root	Worn & cracked at tooth roots	Worn & cracked at tooth roots	Fatigue cracks at tooth root	Broken by torsional fatigue	Broken in brittle manner
Surface finish	Rough at root	Rough at root	Rough at root	Rough at root	Rough at spline root	Reasonable
Material	Not tested	Not tested	Not tested	35CrMo/4135	40Cr	Gr. 60/1060
Gear tooth end round	Large	Large	Large	Small	N/A	N/A
Tooth width	48 mm	48 mm	48 mm	48 mm	N/A	38 mm
Root cracks	Yes	Yes	Yes	Yes	Yes, at splines	Yes
Heat Treatment	Induction hardening	Through-hardened	Not examined	Induction hardening	Through-hardened	Hot rolled
Tooth hardening profile	Flank-and-tooth hardening	N/A	Not examined	Too-and-root hardening	N/A	N/A
Hardness at tooth root/fillet	Below 20 HRC	36 HRC	Not tested	49 HRC	26 HRC at splines	Below 20 HRC

3.1 The Gears

The gears were made with inconsistent metallurgical properties and inadequate strength for the given application. They were also made with a poor surface finish. The inadequate strength of the gears resulting from the heat treatment and the poor gear surface finish contributed to the fatigue failure of the original bottom gear and fatigue cracking in the middle and top gears.

Small gears are either through hardened to a hardness from 30 to 35 HRC for low load applications or induction case-hardened to a surface hardness of 55 to 58 HRC for high load applications. A carburization case-hardening to a 60 HRC range is required for higher load applications.

3.1.1 Mid-gear

The mid-gear was found to be a through-hardened gear with a hardness of 36 HRC, which is considered suitable for low load applications. However, the gear had been severely worn and suffered substantial material flow on the drive flanks in the hoist operation. This means that the hoisting is a high load application. Therefore, the through-hardened mid-gear was not adequate for the application. This high load relatively to the hardness of the gear would have been a primarily contributing factor to the fatigue cracking at the tooth fillet.

3.1.2 Broken Bottom Gear

The broken bottom gear was flank-and-tooth hardened. In this hardening pattern, the root is not hardened and the transition zone of the tooth hardening is at the fatigue critical fillet/root areas (previously shown in **Figure 33**b). This tooth hardening pattern is used for wear resistance applications where fatigue resistance is not a concern. However, fatigue resistance is a key concern in addition to wear in the hoist gear application. With a hardness less than 20 HRC at the fatigue critical fillet/root areas, this gear is the most vulnerable to fatigue cracking among all the gears. This inadequate tooth hardening was the primary cause of its fatigue failure.

The fatigue cracking on this gear might have occurred long ago as evidenced by the severe corrosion of the fracture surface.

It is worthwhile noting that, despite tooth hardening, the hardness of the broken bottom gear had low hardness (35 to 49 HRC) on the hardened flanks. This low hardness was caused by inadequate induction hardening that resulted in the presence of free ferrite grains. This insufficient hardness resulted in severe material flow on the drive flanks of this gear. In addition, the gear might be made of a 35CrMo steel (if it was the same type as the replacement gear). This steel does not contain a sufficient amount of carbon to achieve a higher hardness during induction hardening.

3.1.3 Top Gear

The top gear was found to have fatigue crack indications on the tooth fillet/root areas. The heat treatment and metallurgical qualities of this gear was not examined. Because it has sustained severe wear, the hardness on the tooth flanks is not expected to be sufficient for the application.

In addition, its surface finish was the same as the other gears. Therefore, it might have sustained fatigue cracking as a result.

3.1.4 Replacement Gear

The replacement gear, which was apparently from a different batch than the other gears as evidenced by its different chamfer on the end round, was tooth-and-root hardened with hardness varied from 49 to 52 HRC. In tooth-and-root hardening, the entire tooth and the root are induction hardened (see **Figure 39**b), which provides good wear resistance on the flanks and fatigue strength at the tooth root. This gear is considered to have the best metallurgical quality of all the gears.

Despite a good metallurgical quality, the replacement gear suffered fatigue cracking in less than a month in service. This was likely because the newly installed gear was forced to take most of the load among the three gears due to severe wear on the middle and top gears.

3.1.5 Poor Surface Quality and Fatigue Cracking

All of the gears exhibited a fairly rough surface finish, particularly at the fatigue critical tooth root/fillet areas. The rough surface finish facilitated fatigue cracking at the tooth root/fillet areas, as evidenced by fatigue cracking along the rough machining marks previously seen in **Figure 29**. The rough surface finish would have also contributed to the fatigue failure of the original bottom gear and fatigue cracking in the middle, top and replacement gears.

3.2 Rack Failure

The rack section was found to be made of a hot rolled 1060 steel with a low hardness. This steel would have a low tensile strength and low fracture toughness. However, no evidence was observed on the rack to suggest that its hardness was insufficient for the given application (note that there was not significant material flow on tooth driven flanks). The severe material flow on the teeth adjacent to the fracture was almost certainly caused by the failure of the bottom gear and the failure of the bottom gear shaft.

It has been concluded that fatigue cracking on the original bottom gear had occurred a long time ago. Continuous operation with a broken tooth on the bottom gear would have imposed an impact loading on the rack teeth in each gear revolution. The rack has the smallest cross section at the bolt hole. Given the low fracture toughness of the rack material, it was most likely that the brittle rack failure at the bolt hole was caused by an impact load resulting from continuous operation of the bottom gear with a broken tooth.

3.3 Broken Shaft

The shaft on the bottom gear was made of a Chinese Grade 40Cr steel that was quenched and tempered to a 26 HRC (270 HV 500g) hardness. The shaft failed by rotational fatigue cracking in its splined section. The cracking would have started fairly recently as evidenced by its relatively new fracture appearance.

The shaft would not have sustained severe fatigue cracking at the time the replacement gear was installed. However, this cannot rule out the possibility of early stage fatigue cracking on the splined gear. At least, the shaft would have suffered some damage from repeated impact loading resulting from continuous operation of the bottom gear with a broken tooth.

After the replacement gear was installed, the bottom gear would have been forced to take a greater share of the load among the three gears, due to more wear on the existing gears. Therefore, the bottom gear shaft would have been subjected to higher than expected torsional load. This would result in the observed torsional fatigue failure.

3.4 Sequence of Failures

As discussed above, fatigue cracking in the original bottom gear had started long ago. This gear would have failed first.

The gear failure would have generated impact load on the rack teeth, and this resulted in the rack failure. The rack failure might not be noticed at the time of the bottom gear replacement.

The bottom gear shaft likely had sustained some damage after the original bottom gear lost its tooth. Increase load on the replacement gear would have accelerated the fatigue cracking and resulted in ultimate failure of the shaft.

4.0 CONCLUSIONS AND RECOMMENDATIONS

1. The original bottom gear failed by fatigue cracking that had started long ago. The fatigue failure of the original bottom gear was caused by the use of a gear having inadequate wear and fatigue resistances for the application.

2. The middle gear was through-hardened, as opposed to tooth hardened. It sustained severe wear and suffered fatigue cracking due to inadequate wear and fatigue resistances for the application.

3. The top gear sustained severe wear and suffered fatigue cracking. Although its metallurgical quality was not examined, it was expected to have inadequate wear and fatigue resistances for the application.

4. All gears exhibited fairly rough surface finishes. This would have also contributed to the fatigue failure and cracking in the gears.

5. The replacement gear exhibited a better tooth hardening pattern and higher hardness on the fillet/root area. However, it suffered fatigue cracking after only a month in service. This premature fatigue cracking was likely due to excessively high load due to unbalanced load sharing among the gears. Rough surface finish was also a contributing factor to the fatigue cracking.

6. The brittle failure of the rack section was caused by an impact load by the bottom gear after its tooth broke off.

7. Torsional fatigue cracking of the bottom gear shaft might have started after the original bottom gear suffered a broken tooth. The cracking might have been accelerated after installation of the replacement gear which took a higher share of load, and the shaft ultimately broke by torsional fatigue cracking a month later.

[redacted]., P.Eng.

Note: Unless otherwise instructed, we shall dispose of all parts and test samples sixty days from the date of this report.

ACUREN

APPENDIX

FIGURES 1 - 40

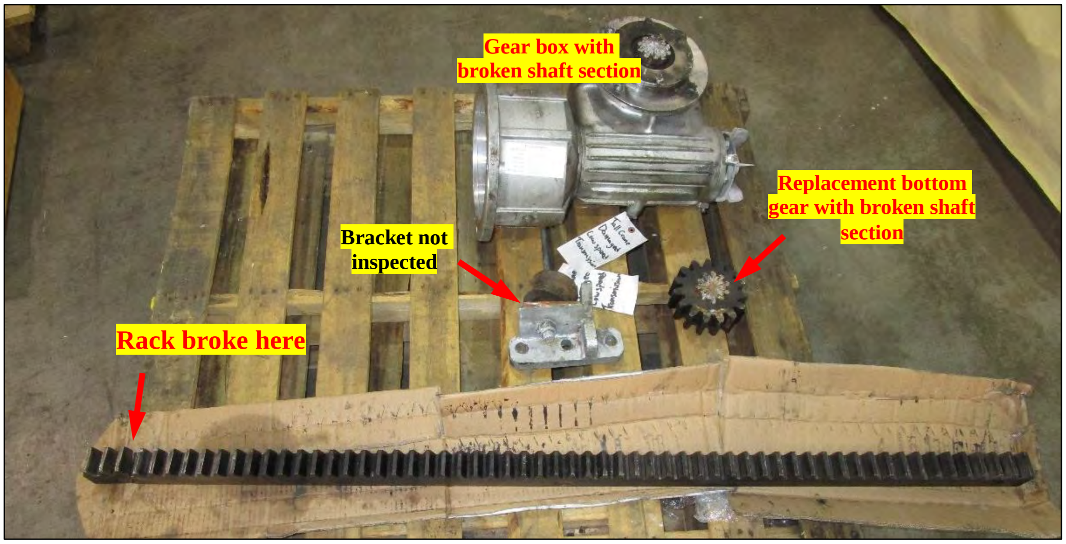

(a)

(b)

Figure 1 Failed components of construction hoist as received.

Figure 2 Name plate on gear box.

(a) Gear box side

(b) Gear side

Figure 3 Fractures of broken bottom gear splined shaft.

Figure 4 The outboard end of splined shaft inside bottom gear.

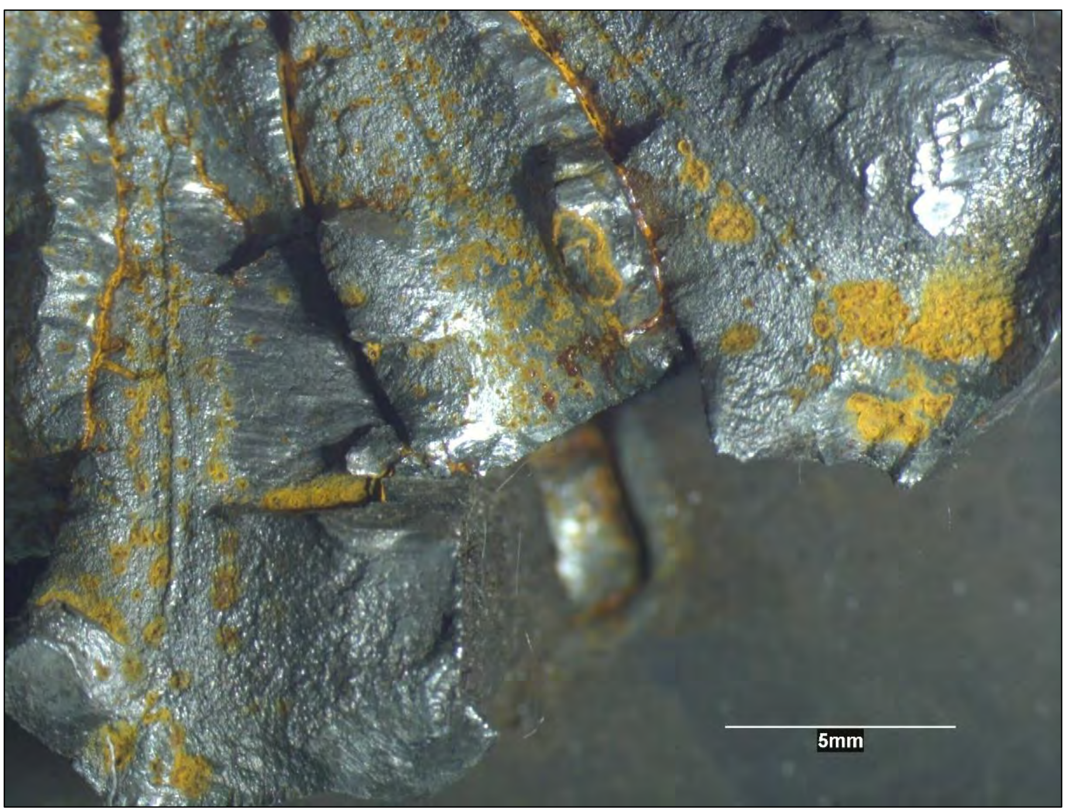

Figure 5 Close up of shaft fracture showing coarse fatigue beach marks.

Figure 6 General appearance of shaft fracture after cleaning.

(a) Before cleaning

(b) After cleaning

Figure 7 General appearance of splined section of broken shaft.

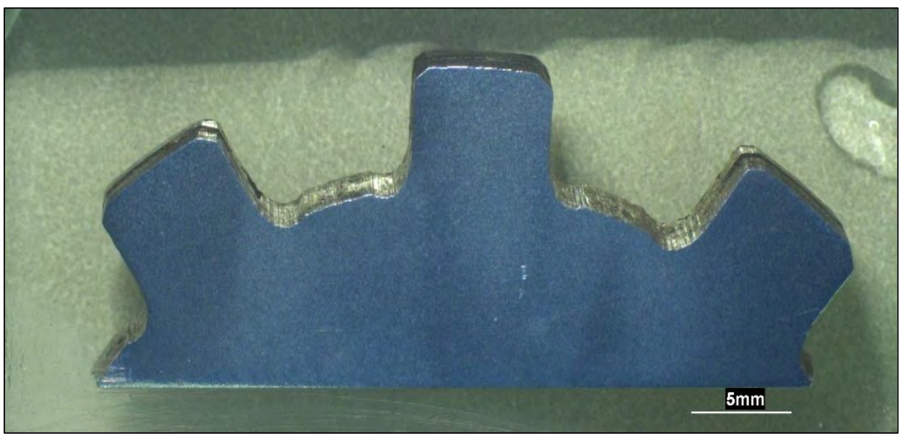

Figure 8 Metallographic specimen of splined shaft.

ACUREN

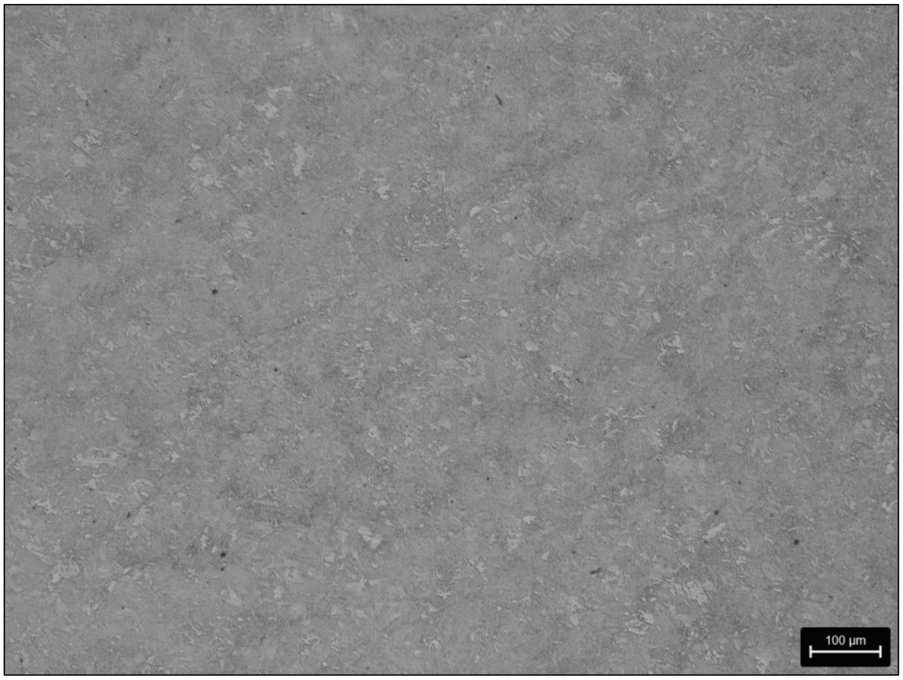

(a) Approximate magnification 100x

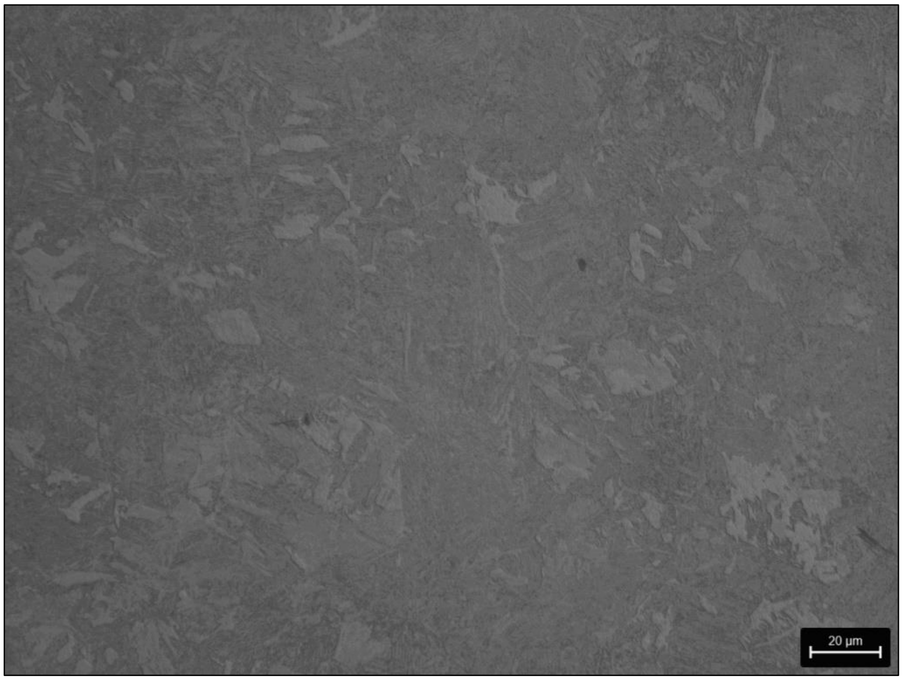

(b) Approximate magnification 500x

Figure 9 General microstructure of splined shaft.

Figure 10 Rack section has bolt hole on each end.

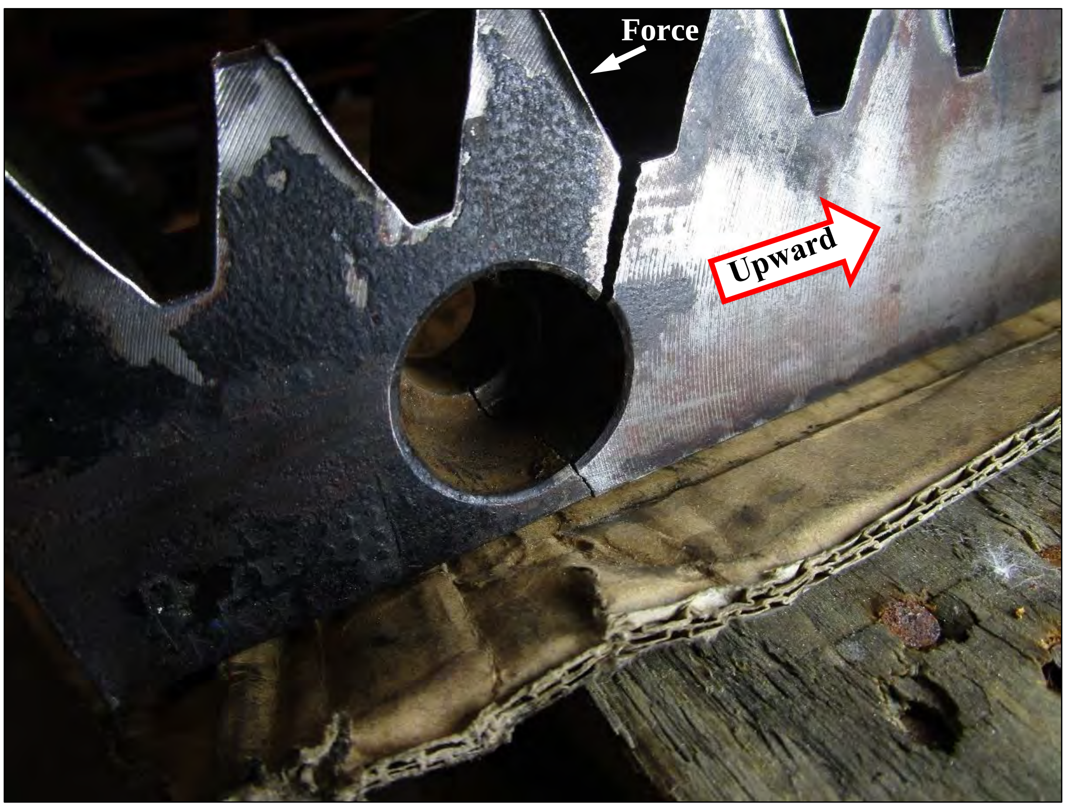

Figure 11 Rack fractured through one of the bolt holes.

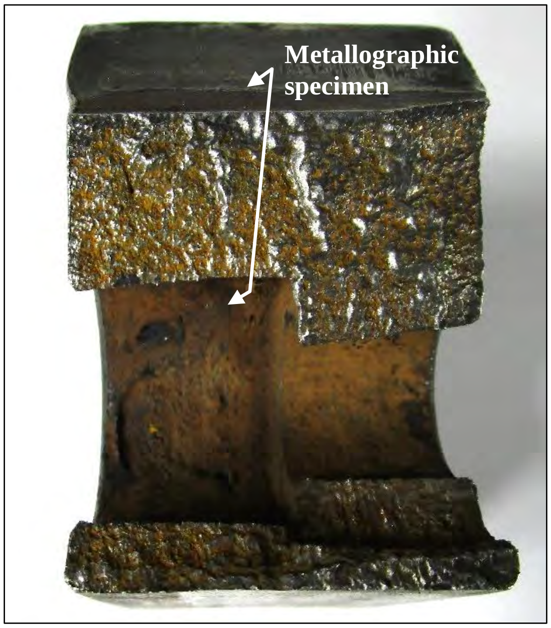

(a) Before cleaning (b) After cleaning

Figure 12 Fracture of rack.

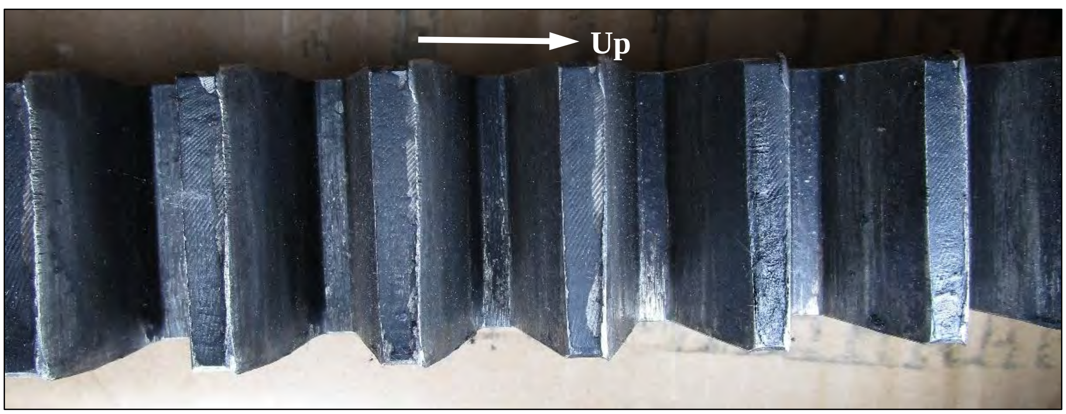

(a) General appearance

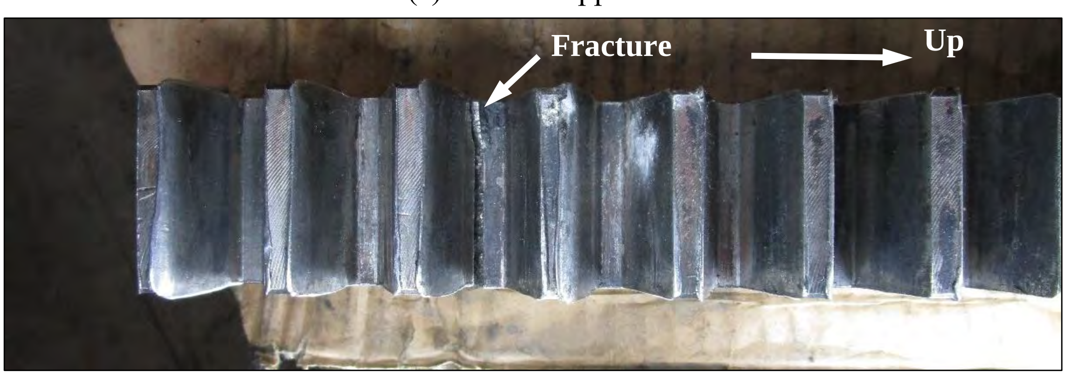

(b) Teeth adjacent to fracture

Figure 13 General appearance of rack teeth.

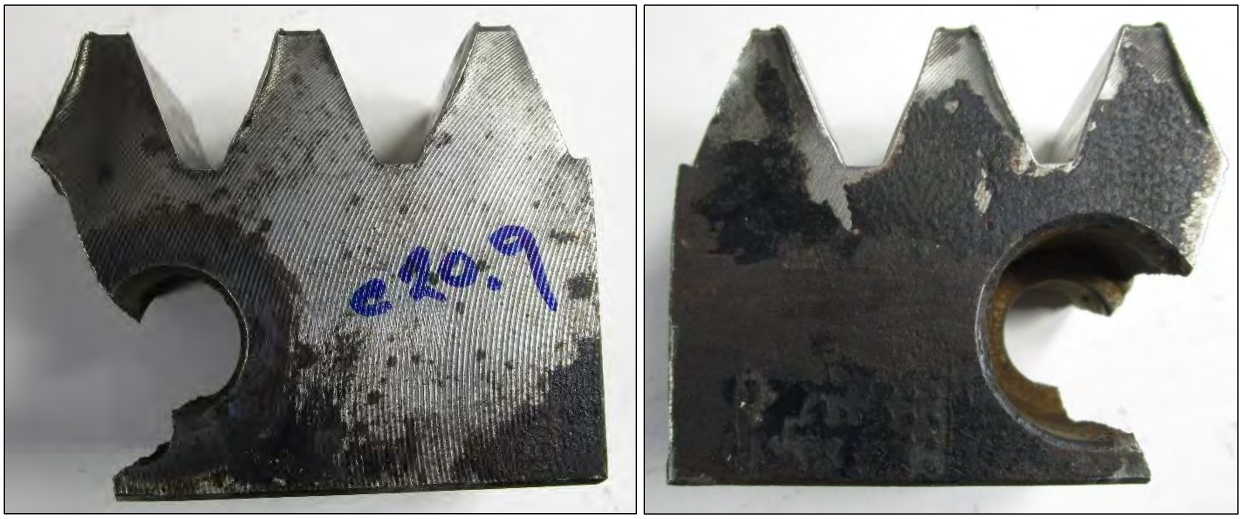

(a) Two side views

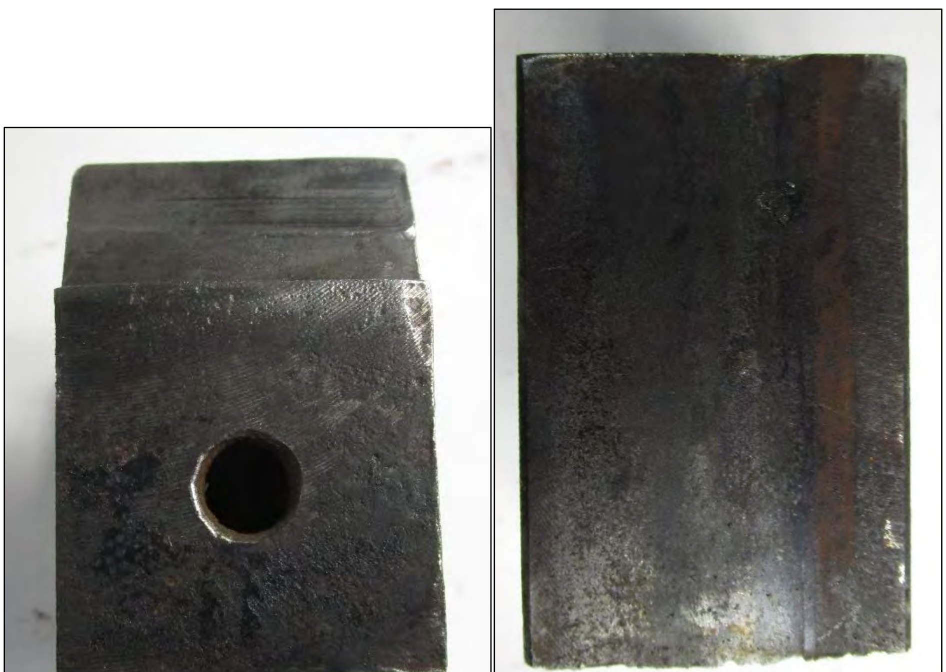

(b) End surface connecting to next rack (c) Bottom surface

Figure 14 General surface appearance of broke away rack piece.

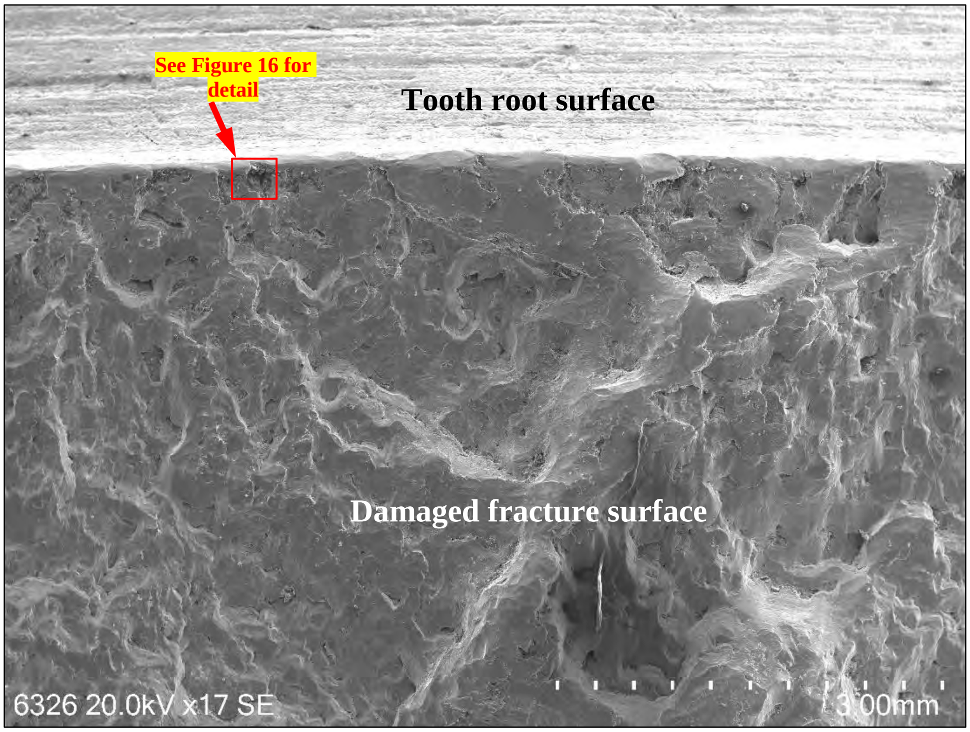

Approximate magnification 17x

Figure 15 SEM image of fracture on rack at origins.

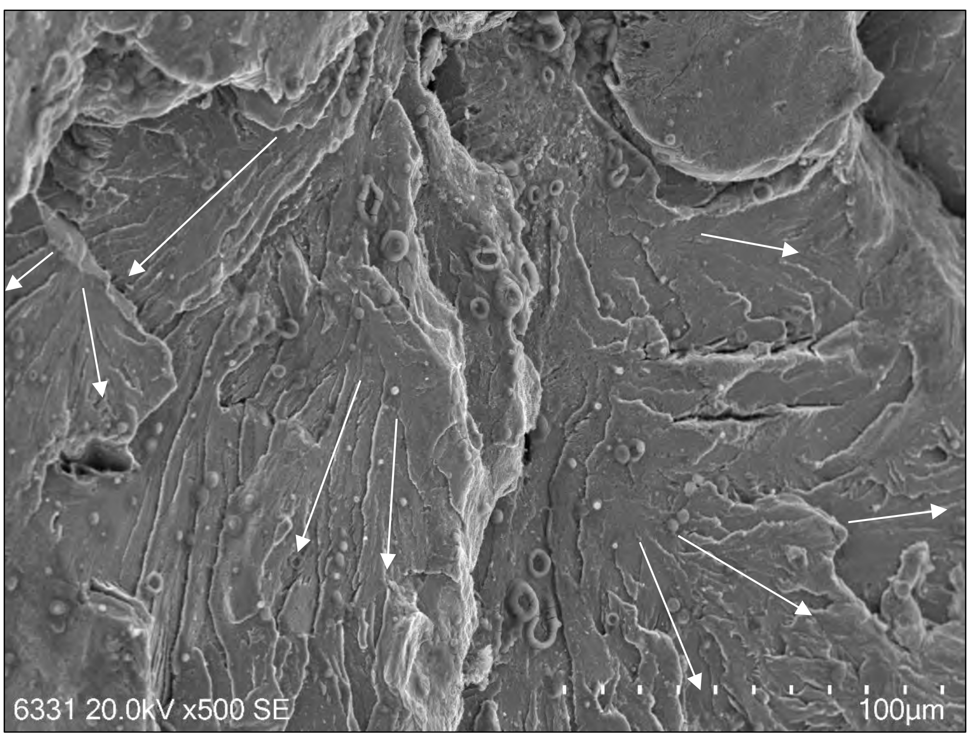

Approximate magnification 500x

Figure 16 Fractography of rack fracture showing brittle cleavage pattern.

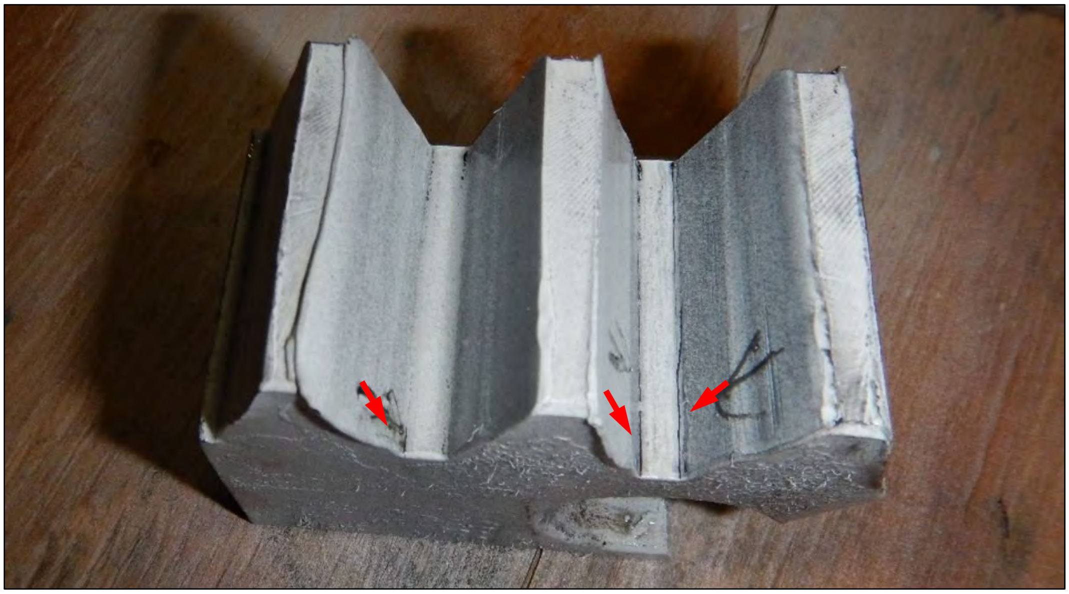

Figure 17 Linear indications along tooth roots adjacent to fracture revealed by MPI

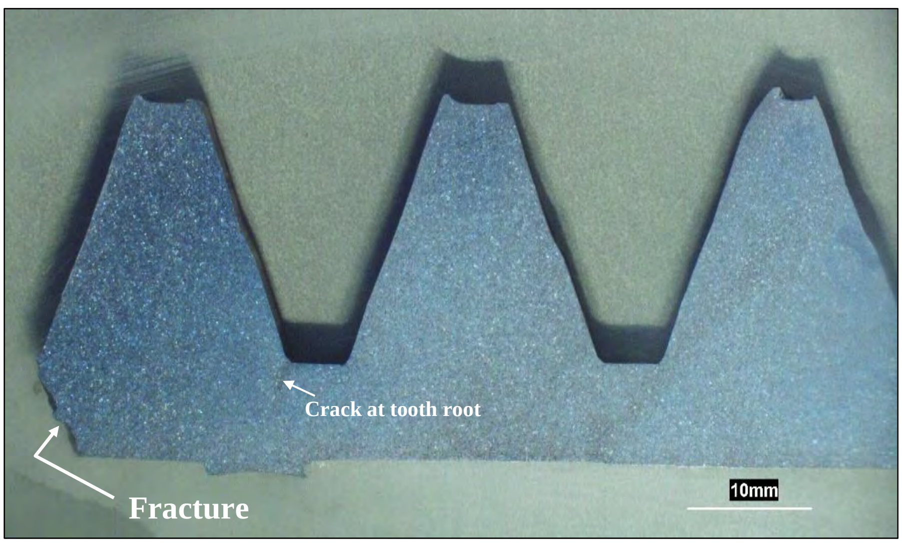

Figure 18 Metallographic specimen of rack across fracture.

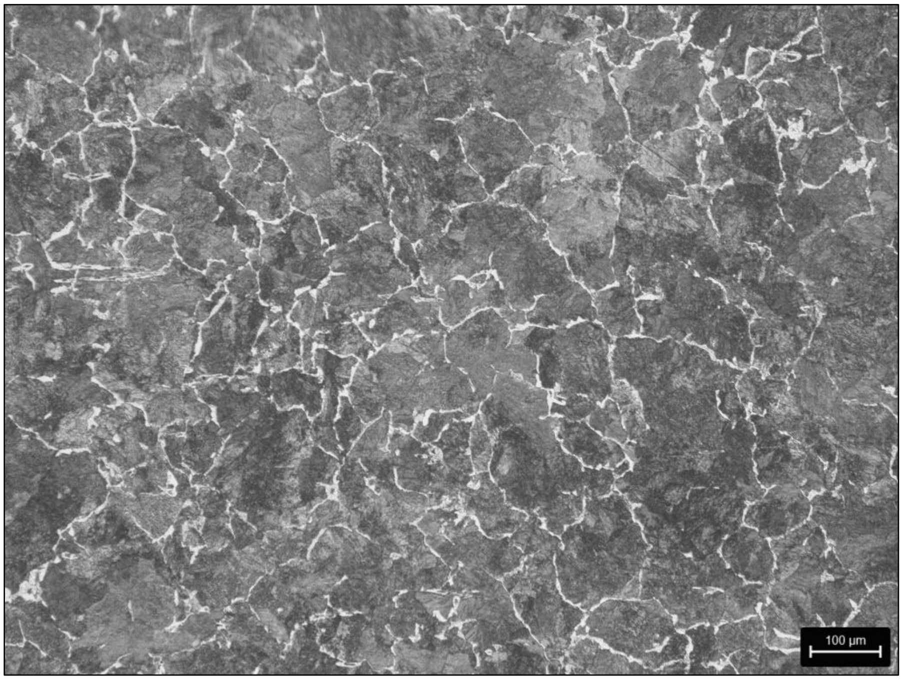

(a) Approximate magnification 100x

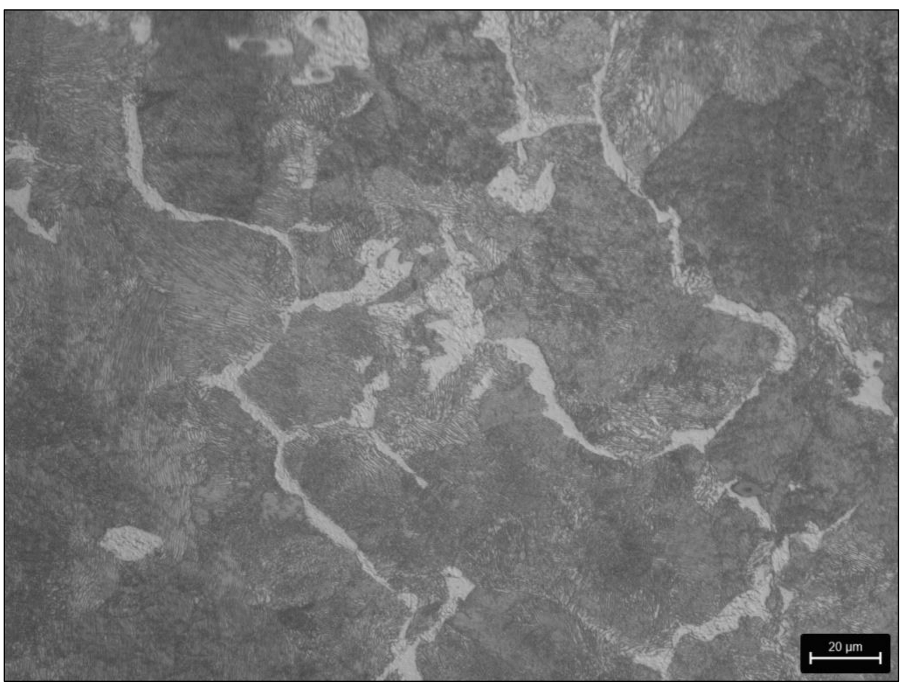

(b) Approximate magnification 500x

Figure 19 General microstructure of rack steel.

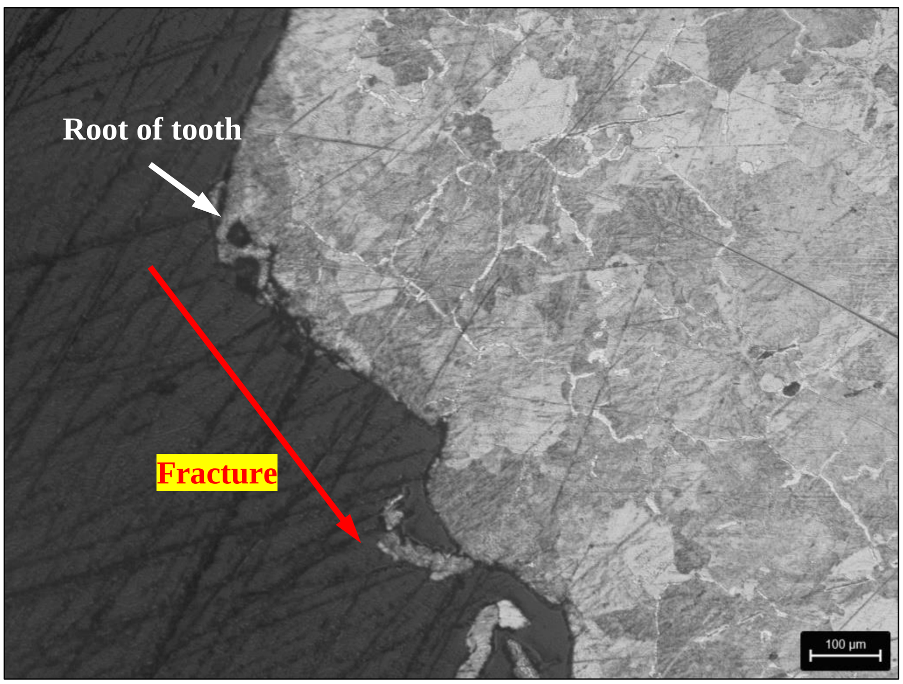

Approximate magnification 100x

Figure 20 Profile of fracture and surrounding microstructure.

Approximate magnification 100x

Figure 21 Profile of large tooth root crack and surrounding microstructure.

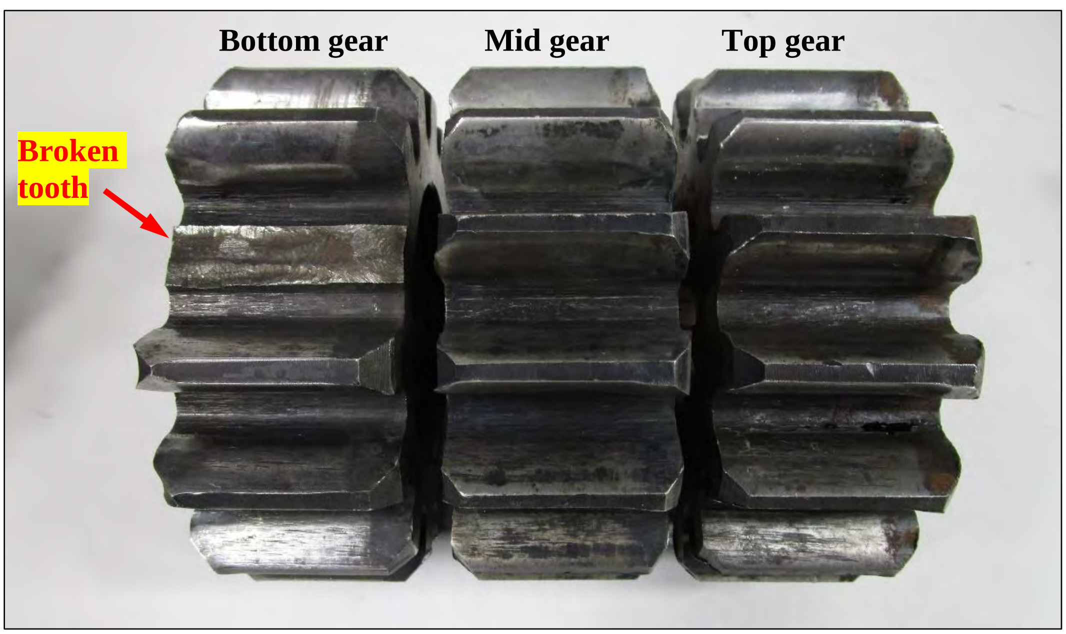

Figure 22 Three original gears as received.

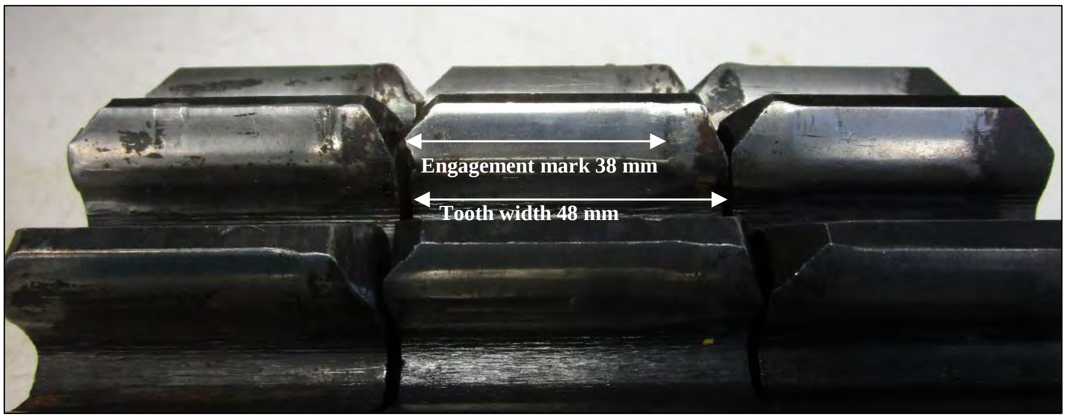

(a) Drive side of teeth.

(b) Non-drive side of teeth

Figure 23 Close up of meshing pattern on original set of gears.

Figure 24 Illustration of meshing teeth of gear and rack.

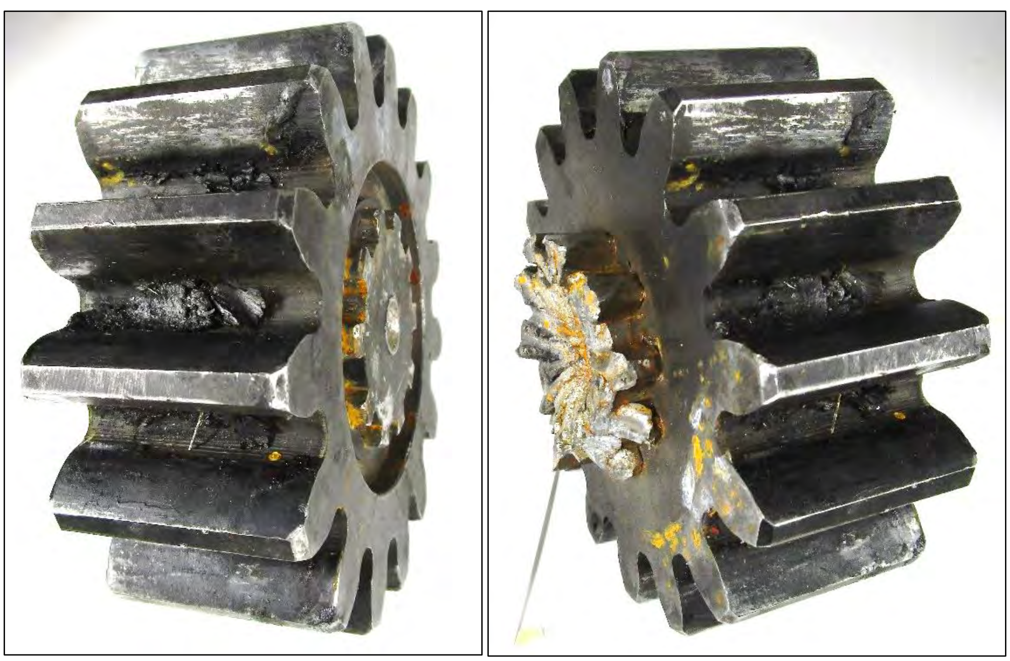

Figure 25 Replacement gear with broken shaft inside.

(a)

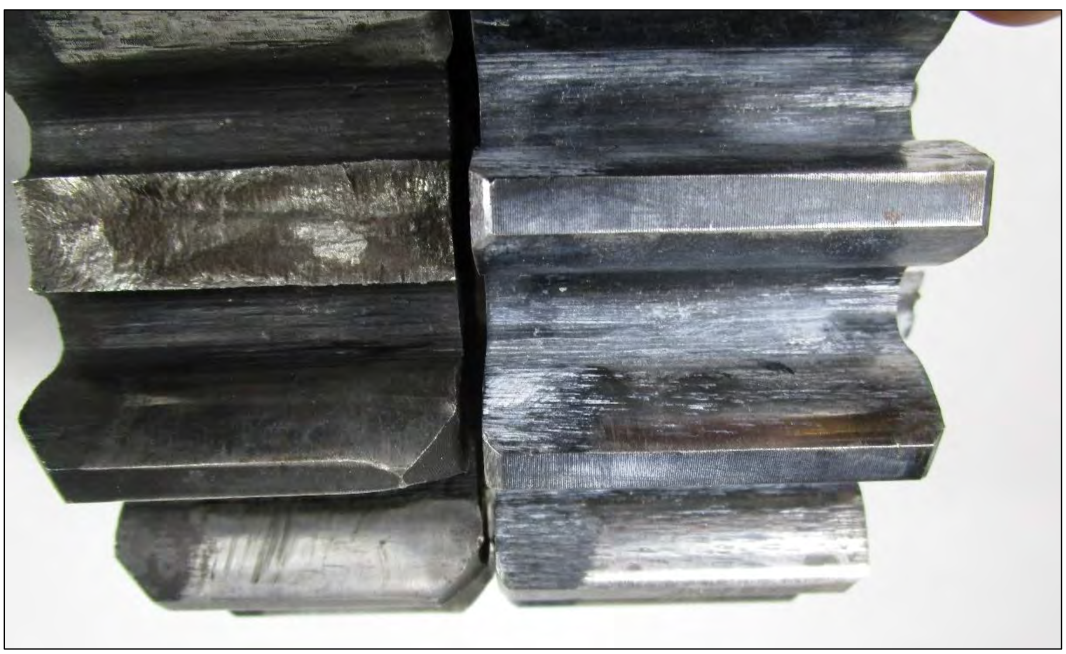

(b)

Figure 26 Comparison of tooth profile of replacement gear and original gear.

ACUREN

(a) Original gears

(b) Replacement gear

Figure 27 Liner indications revealed by MPI inspection.

Figure 28 Broken tooth and its fracture.

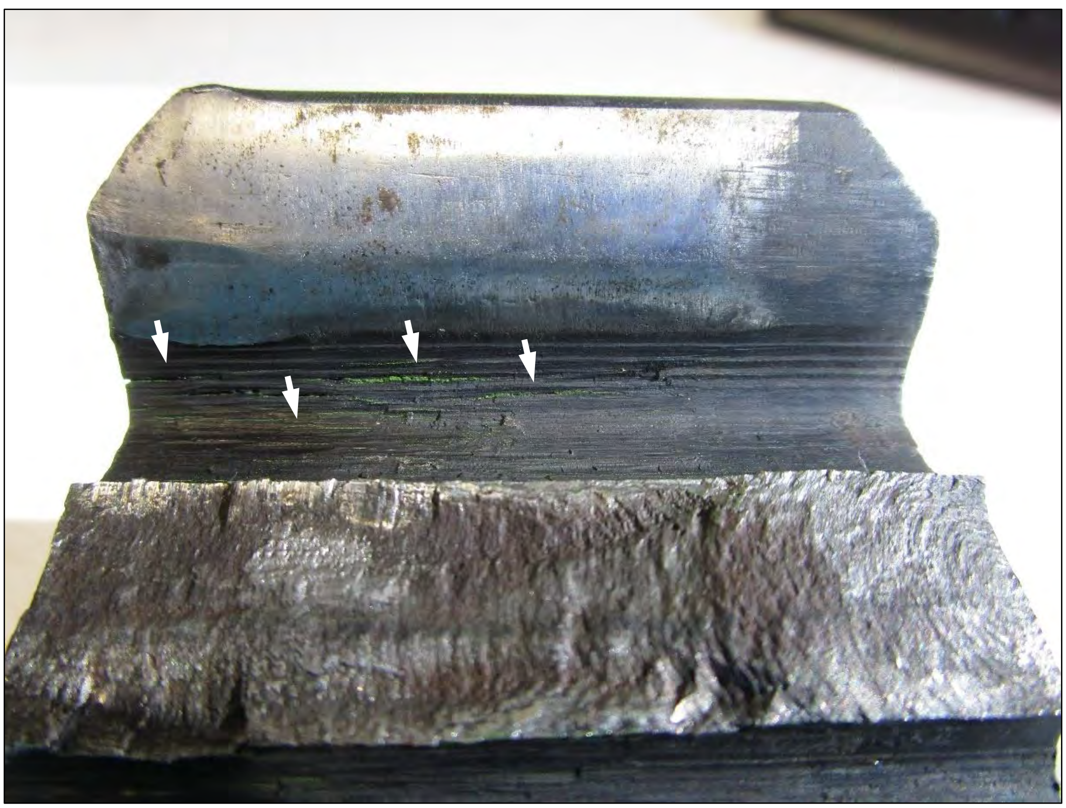

Figure 29 Secondary cracks on rough machined fillet of neighbouring tooth.

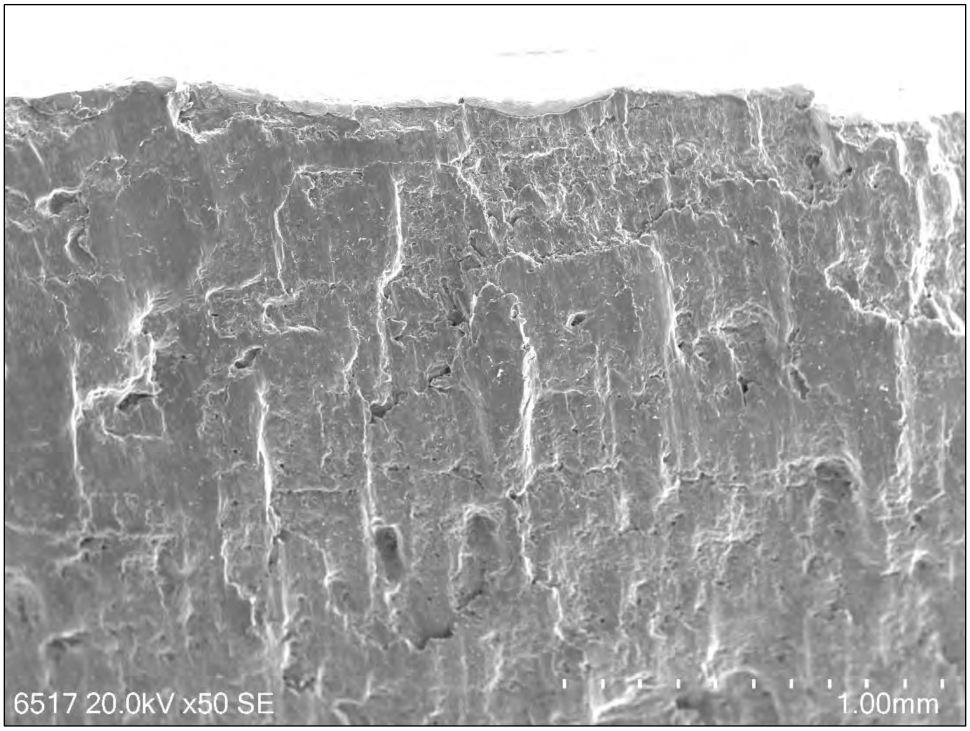

(a) Approximate magnification 50x

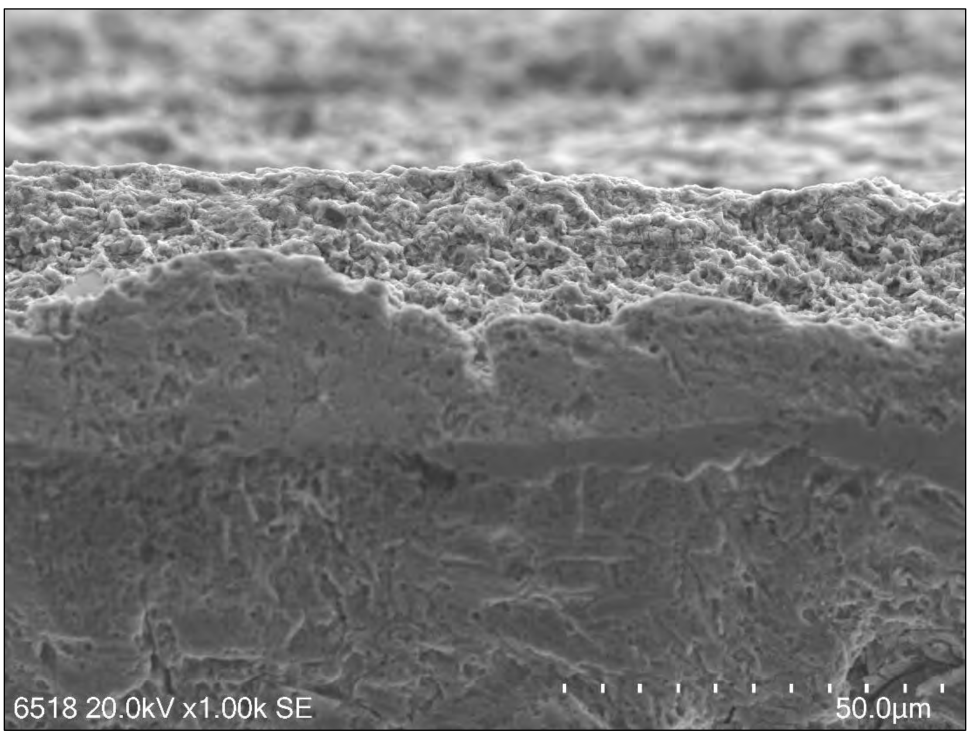

(b) Approximate magnification 1,000x

Figure 30 SEM images of fracture along edge of drive side.

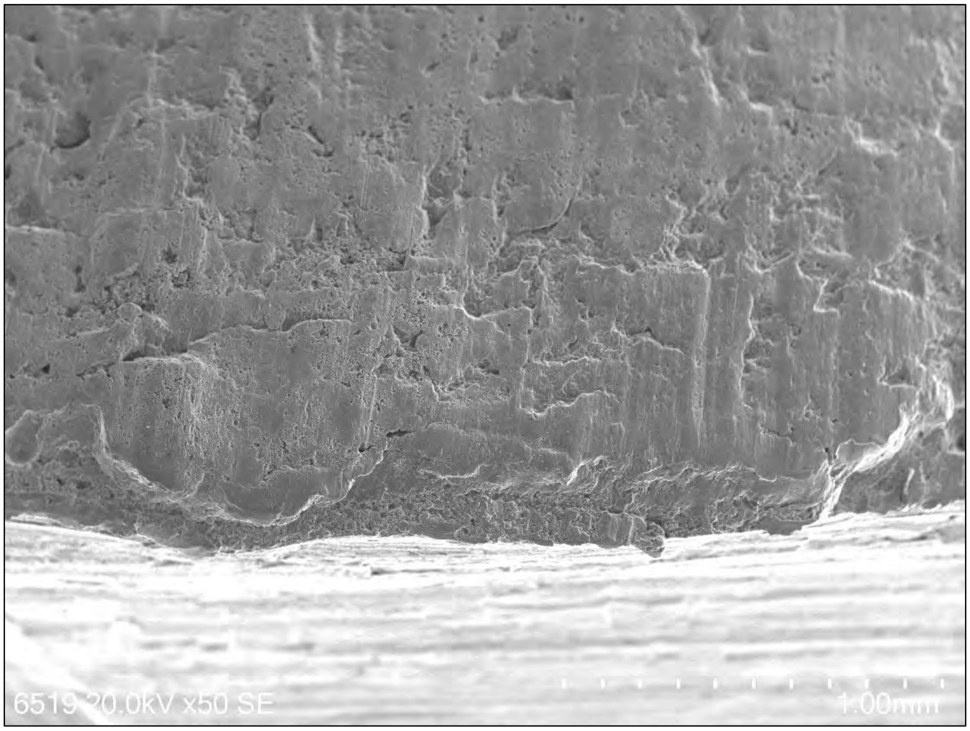

(a) Approximate magnification 50x

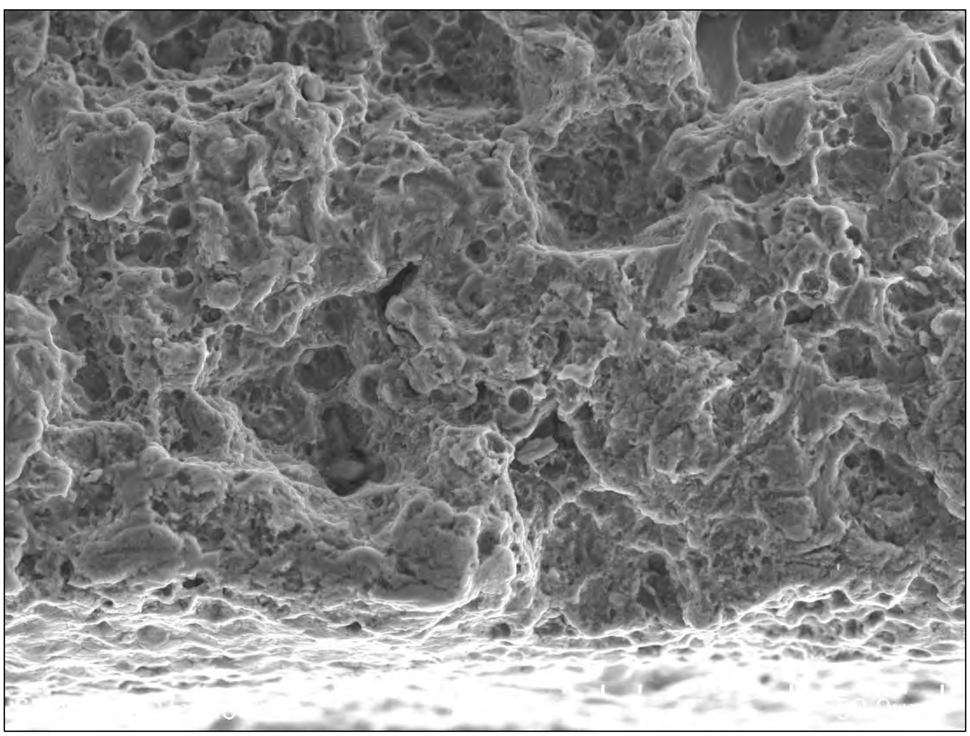

(b) Approximate magnification 1,000x

Figure 31 SEM images of fracture along edge of non-drive side.

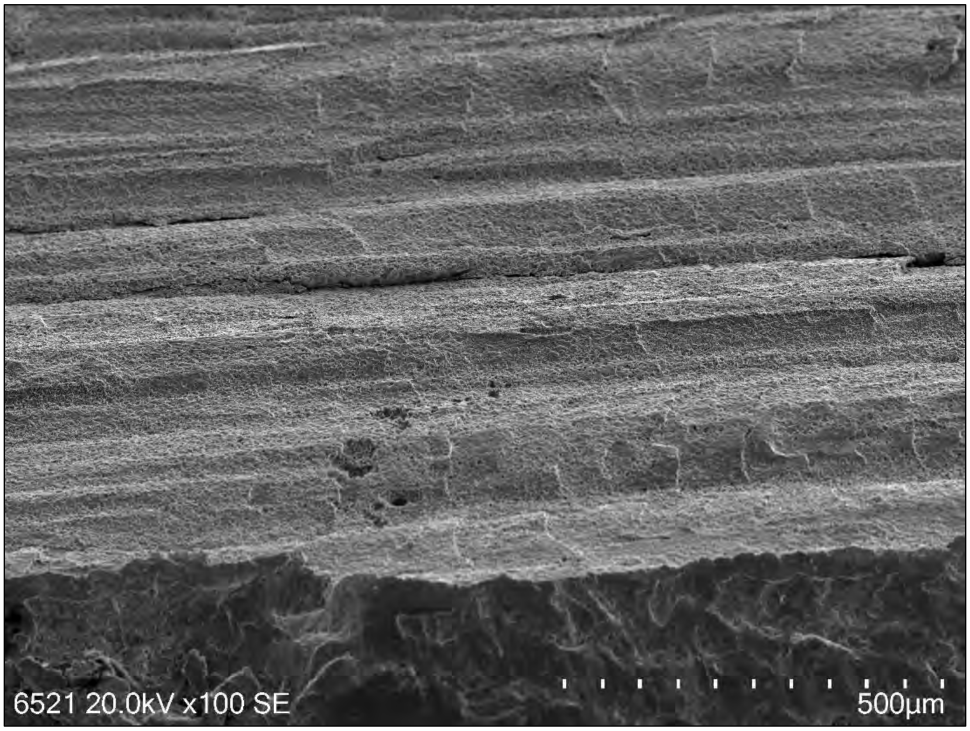

(a)

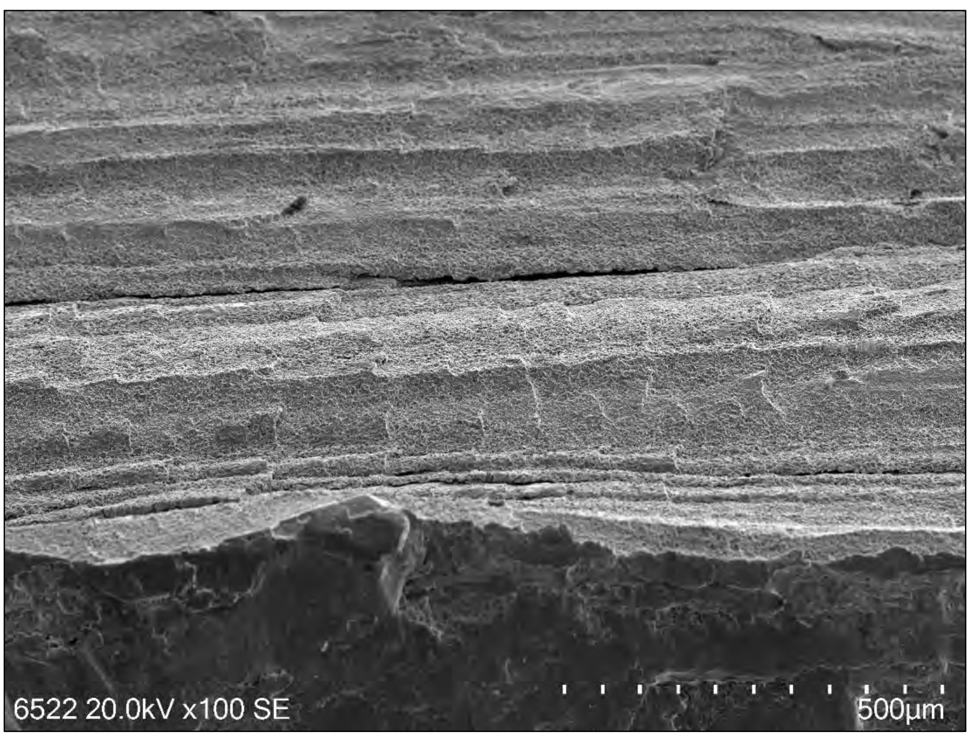

(b)

Figure 32 SEM images of secondary cracks along tooth root on dive side.

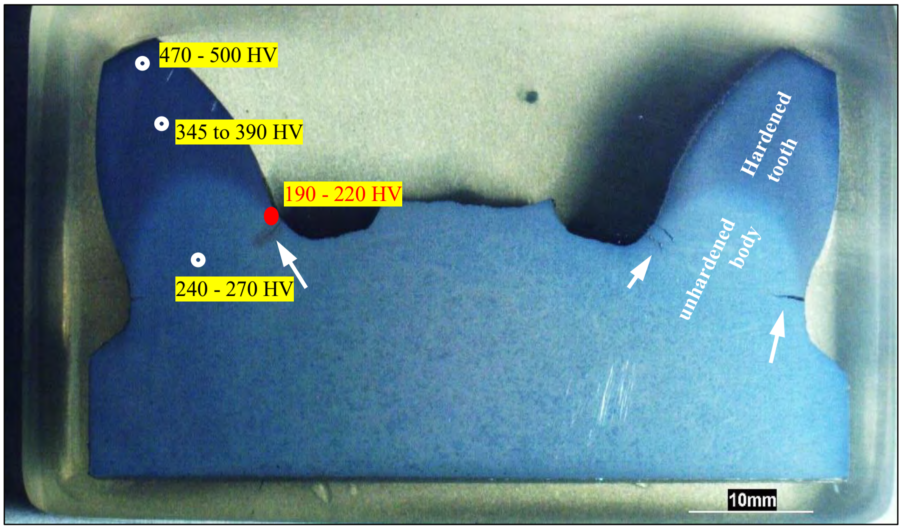

(a) Metallographic specimen

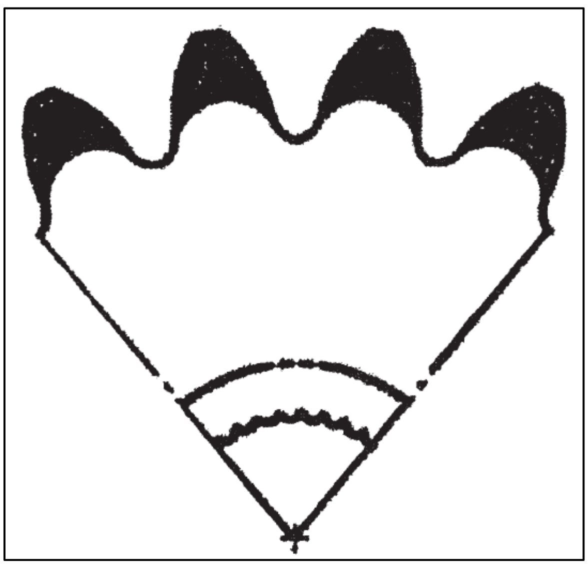

(b) Flank-and-tooth hardening pattern

Figure 33 Metallographic specimen of broken gear across fracture showing flank-and-tooth hardening pattern.

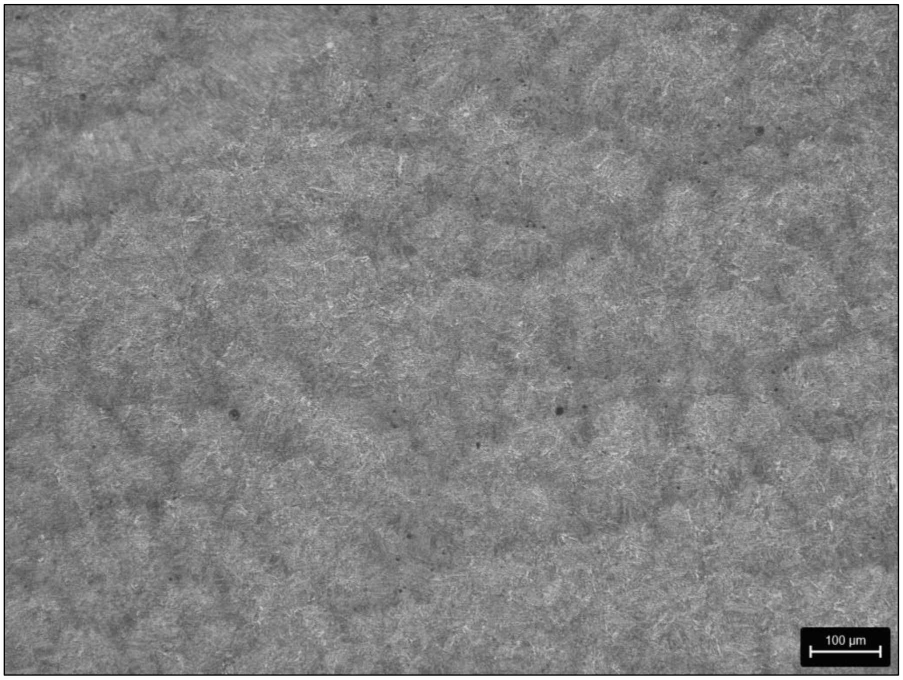

(a) Approximate magnification 100x

(b) Approximate magnification 500x

Figure 34 General microstructure of body of broken gear.

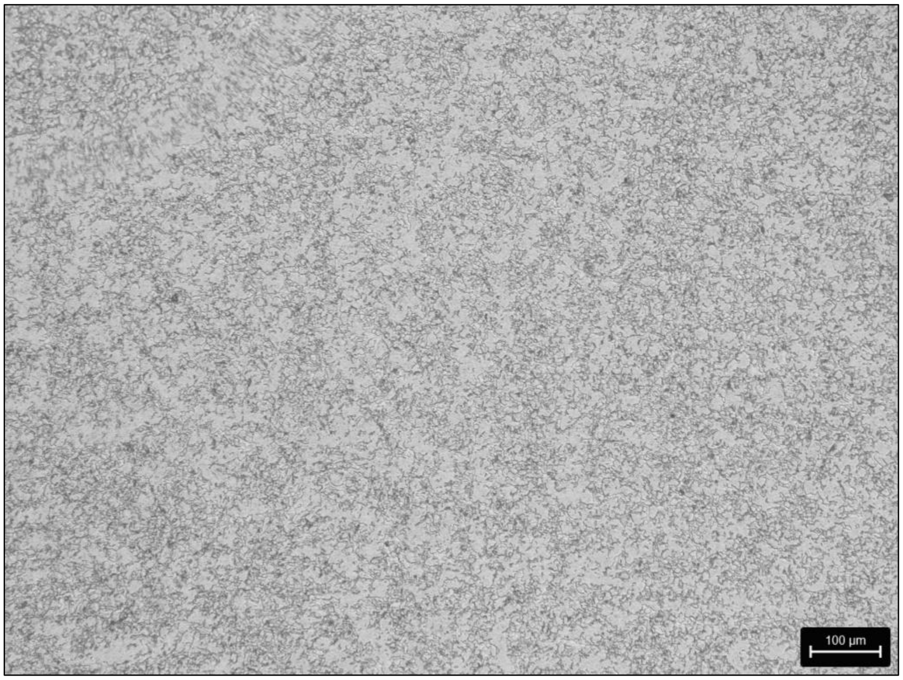

(a) Approximate magnification 100x

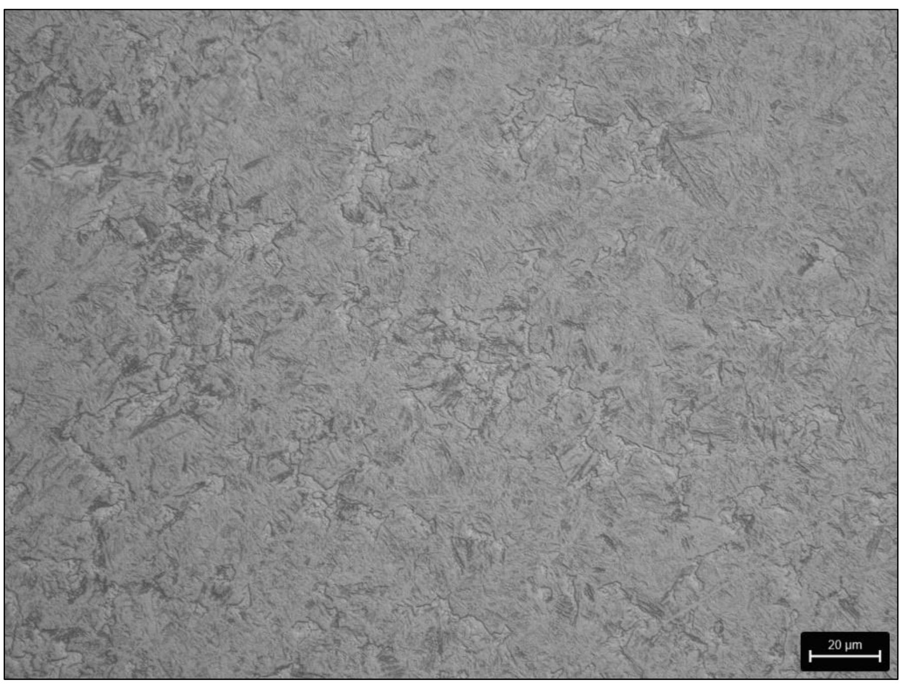

(b) Approximate magnification 500x

Figure 35 General microstructure of tooth in hardened zone, broken gear.

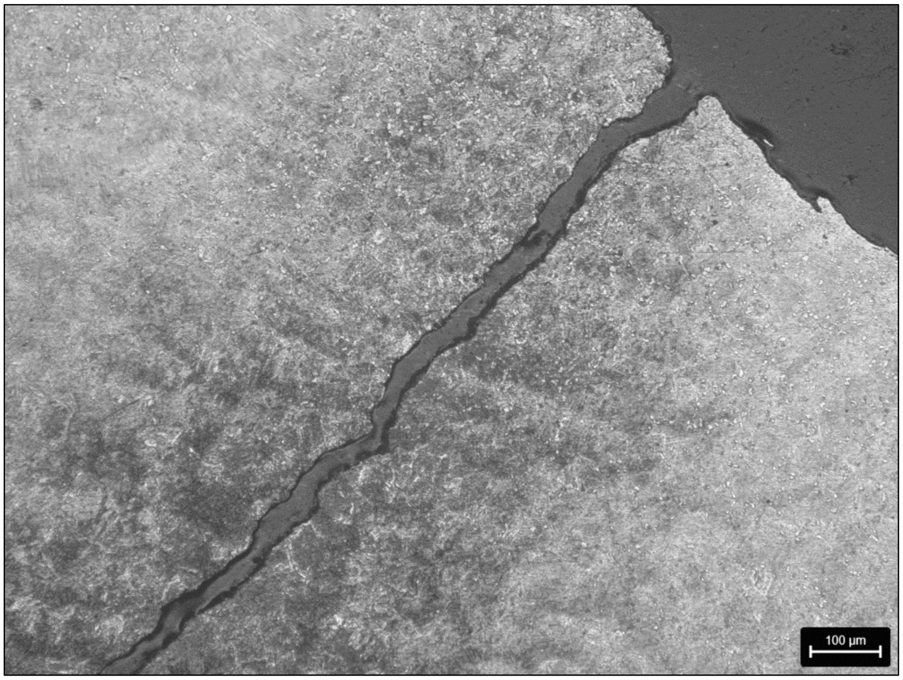

(a) Approximate magnification 100x

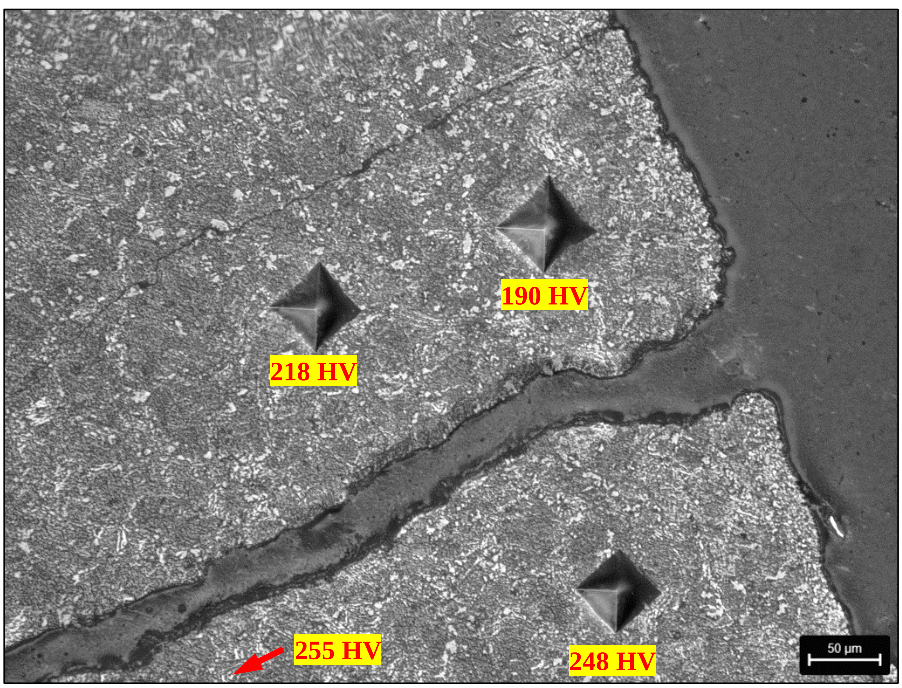

(b) Hardness indents (another location). Approximate magnification 200x

Figure 36 Profile of crack and surrounding microstructures, broken gear.

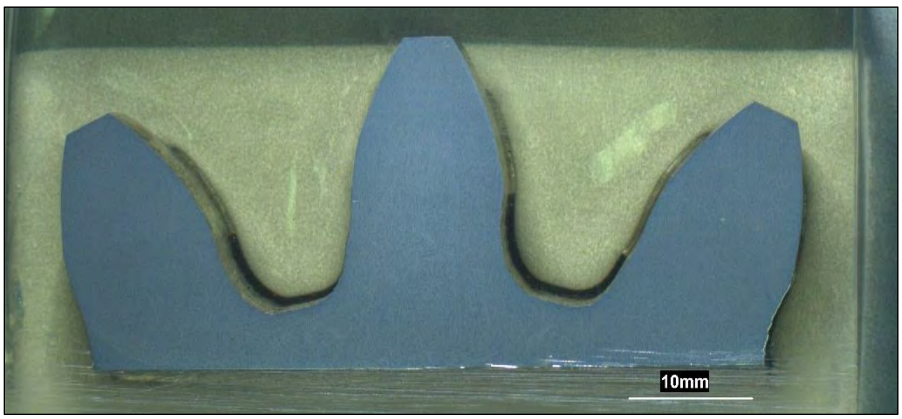

Figure 37 Metallographic specimen of mid-gear showing through-hardened pattern.

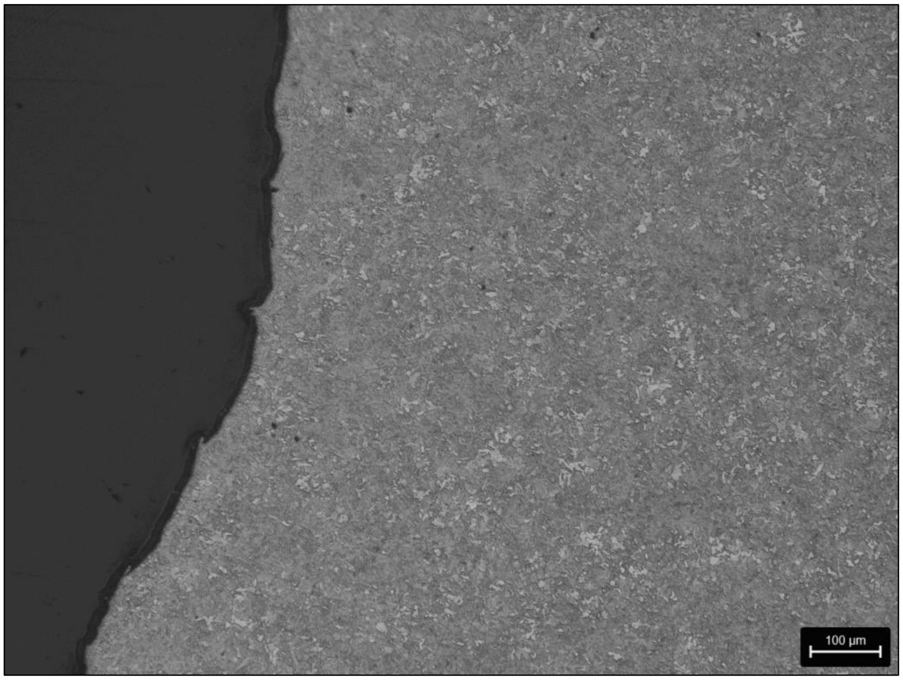

(a) Approximate magnification 100x

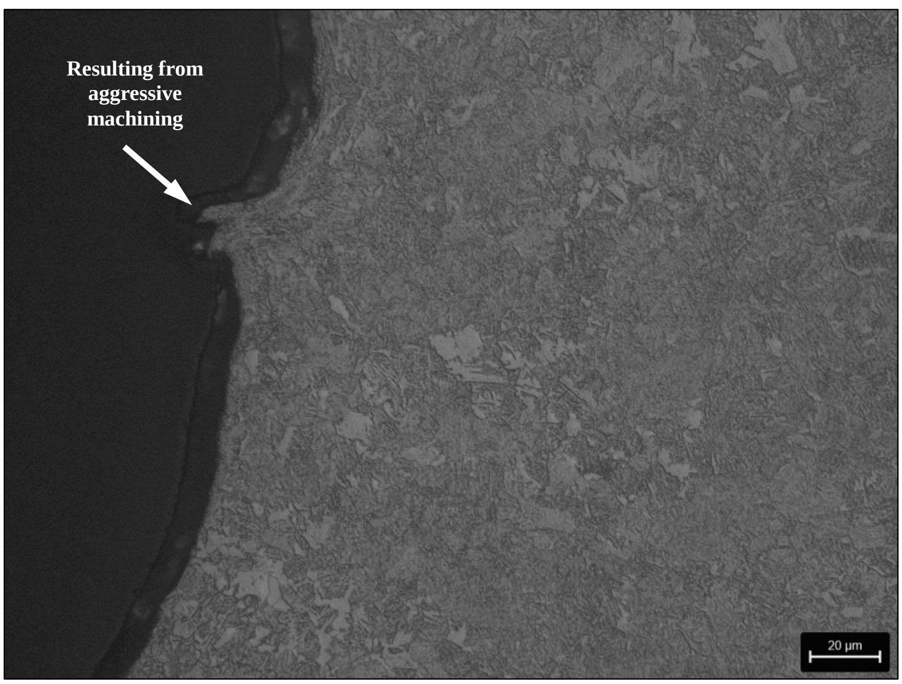

(b) Approximate magnification 500x

Figure 38 Profile of gear root and surrounding microstructure of mid-gear.

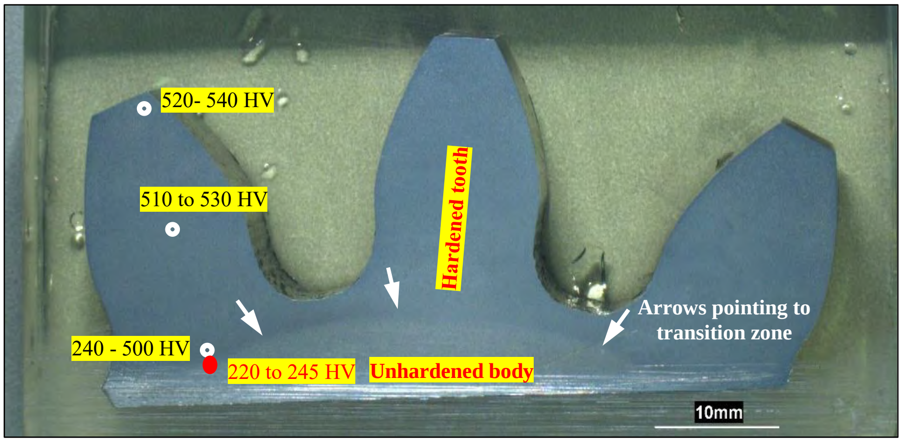

(a) Metallographic specimen

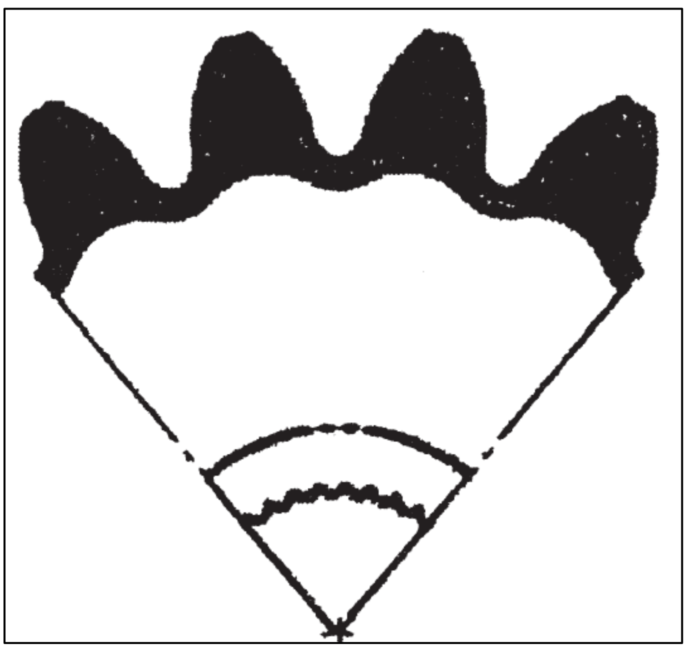

(b) Tooth-and-root hardening pattern

Figure 39 Metallographic specimen of replacement gear showing tooth-and-root hardening pattern.

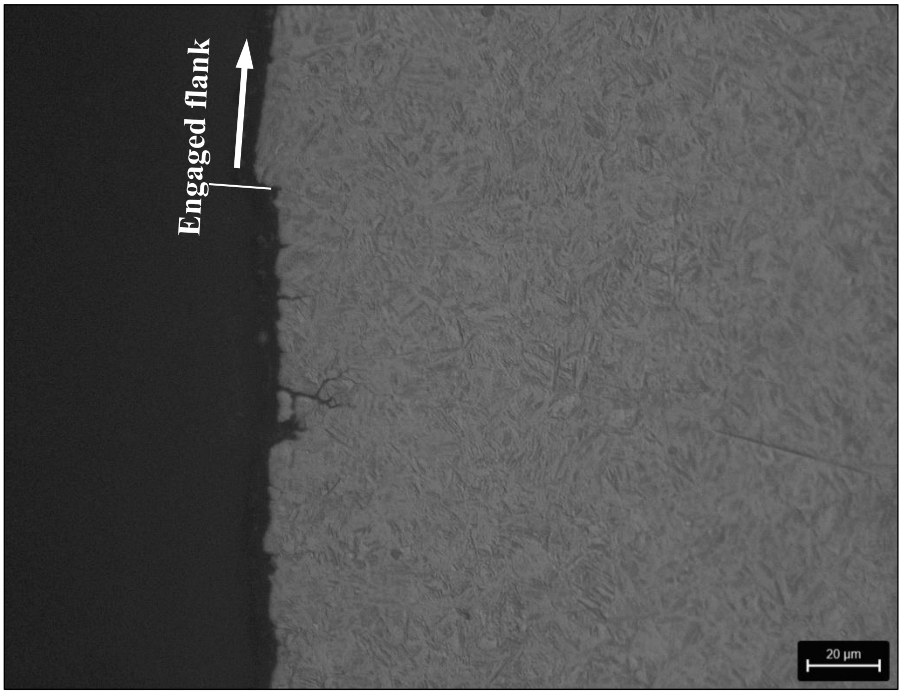

(a) Drive side. Approximate magnification 500x

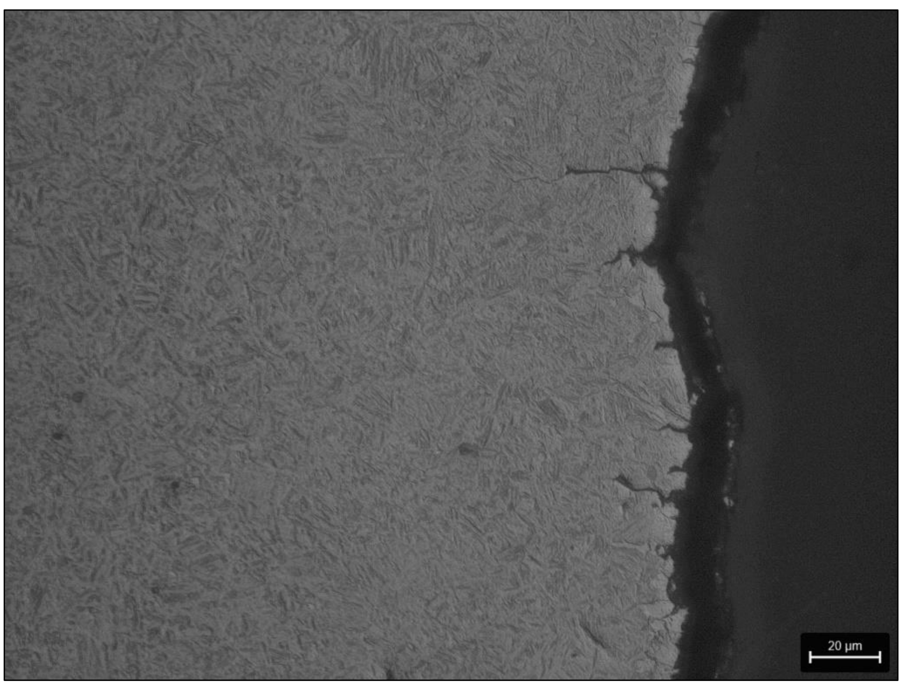

(b) Not-drive side. Approximate magnification 500x

Figure 40 Cracks at tooth fillet and surrounding microstructure of replacement gear.